Tackling fully-heavy tetraquark production with NRQCD factorization

Yingsheng Huang

Central South University

Based on

PRD 106 (2022), 114029; PLB 818 (2021), 136368; CPC 45 (2021), 093101;
PRD 108 (2023), L051501; PRD 110 (2024), 054007; JHEP 09 (2024), 002;
PRD 111 (2025), 054006

May 15th, 2026 @University of Jyväskylä

Outline

1. Exotics and Fully-heavy tetraquarks
2. NRQCD Factorization of T4c
3. Phenomenological applications
4. Summary

Exotics and Fully-heavy tetraquarks

THE FAMILY OF HADRONS

ORDINARY HADRONS

MESONS

BARYONS

EXOTIC HADRONS

TETRAQUARK

PENTAQUARK

HYBRIDS

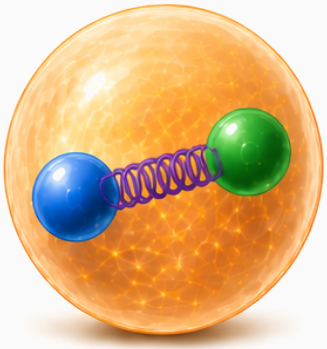

HADRON MOLECULE

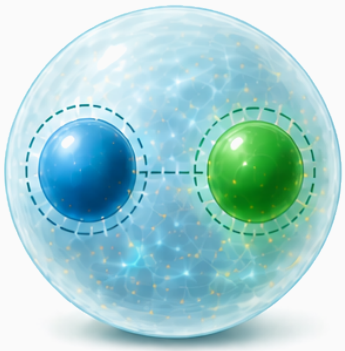

EXOTIC HADRONS Gell-Mann, Phys. Lett. 8, 214 (1964)

- Ordinary hadrons:
  - mesons $|q\bar{q}\rangle$
  - baryons $|qqq\rangle$
- Exotic hadrons:

  not ordinary;
  new quantum numbers,
  anomalous properties, etc.,
  already allowed by the quark model
  - multiquark states: $|qq\bar{q}\bar{q}\rangle$
  - hadronic molecules:
    $|X(3872)\rangle \sim$
    $|D^0\bar{D}^{*0}\rangle + |\bar{D}^0 D^{*0}\rangle$
  - hybrids ($|q\bar{q}g\rangle$), etc.

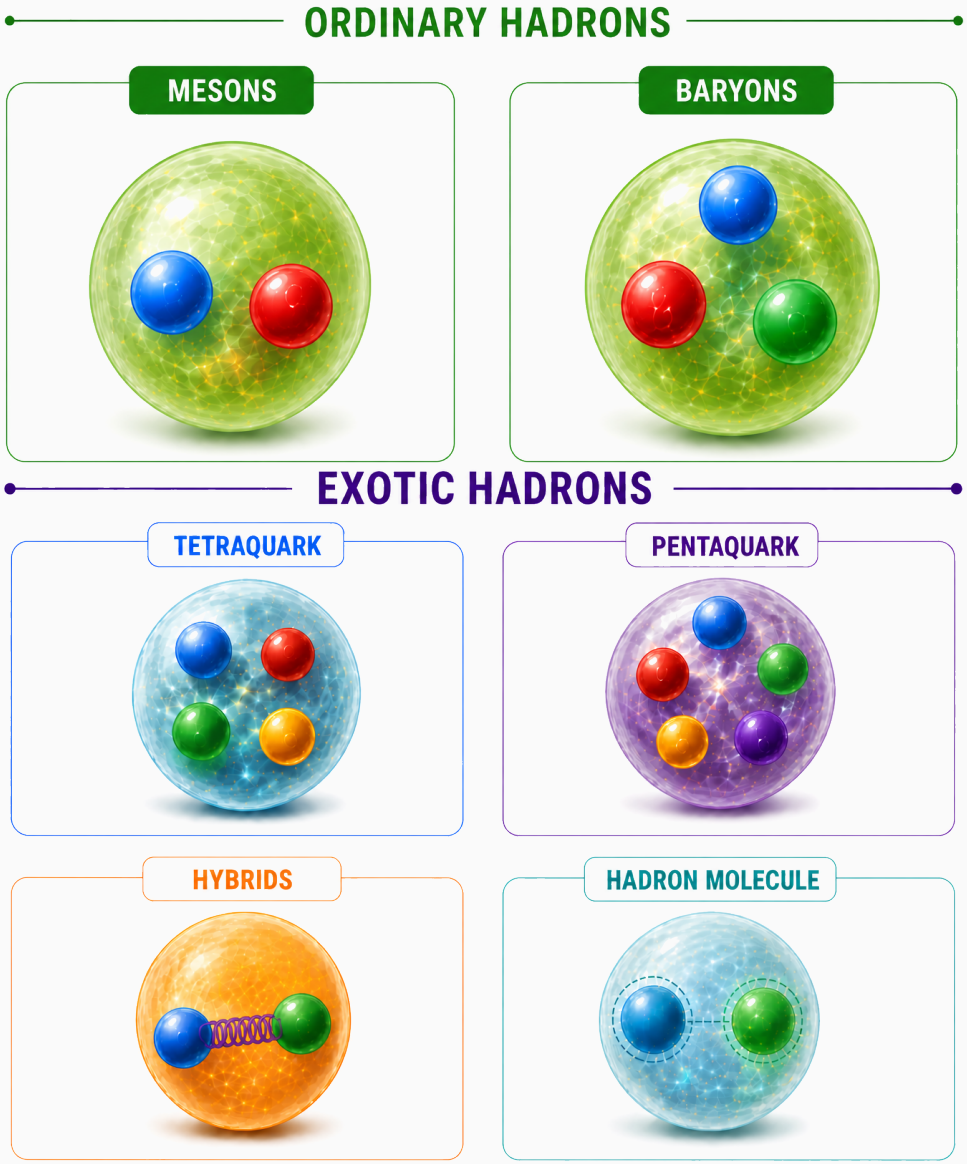

MASSIF OF EXOTIC HADRONS

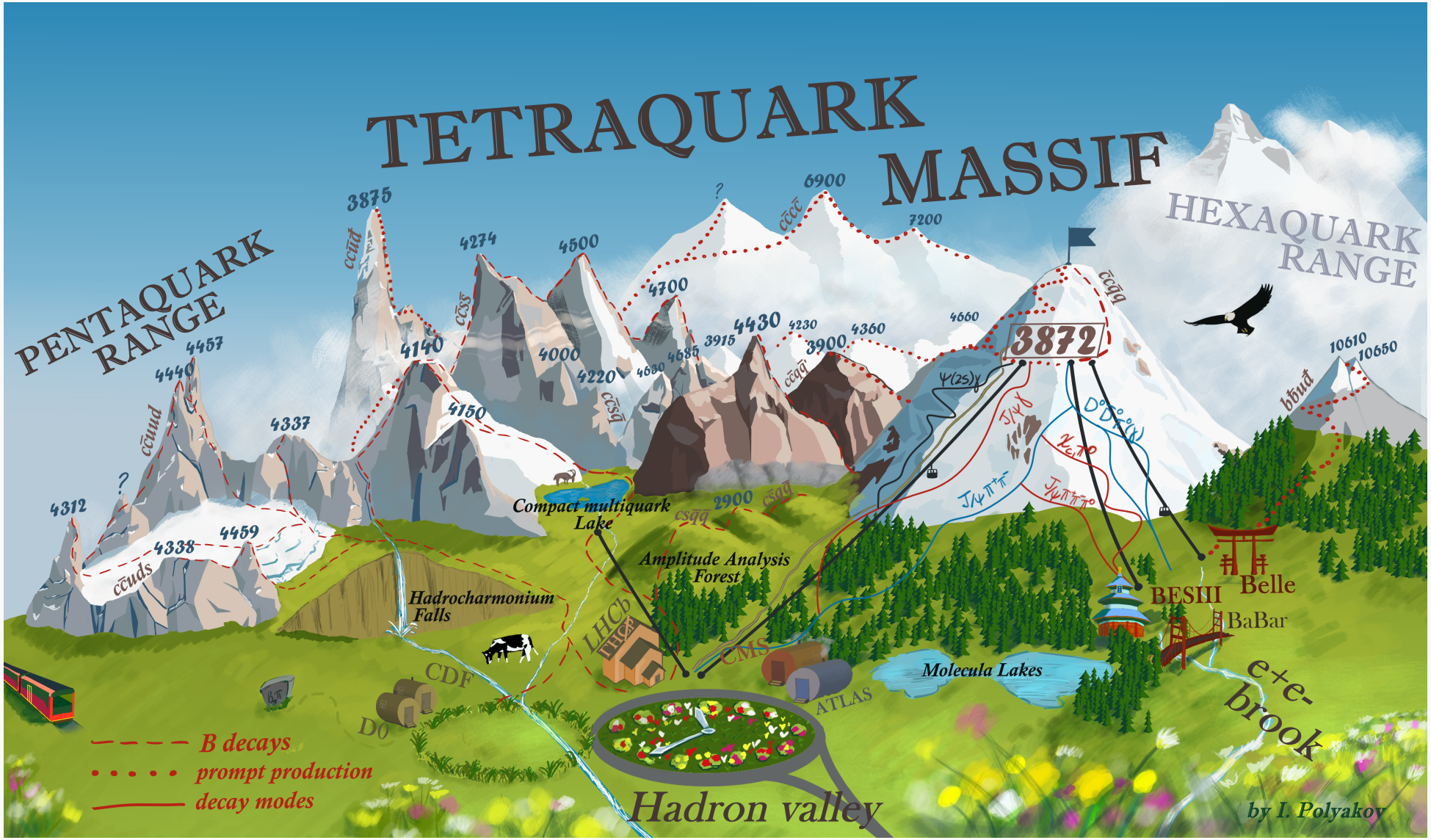

Hüsken et al., Mod.Phys.Lett.A 40 17n18, 2530002 (2025)

MASSIF OF EXOTIC HADRONS

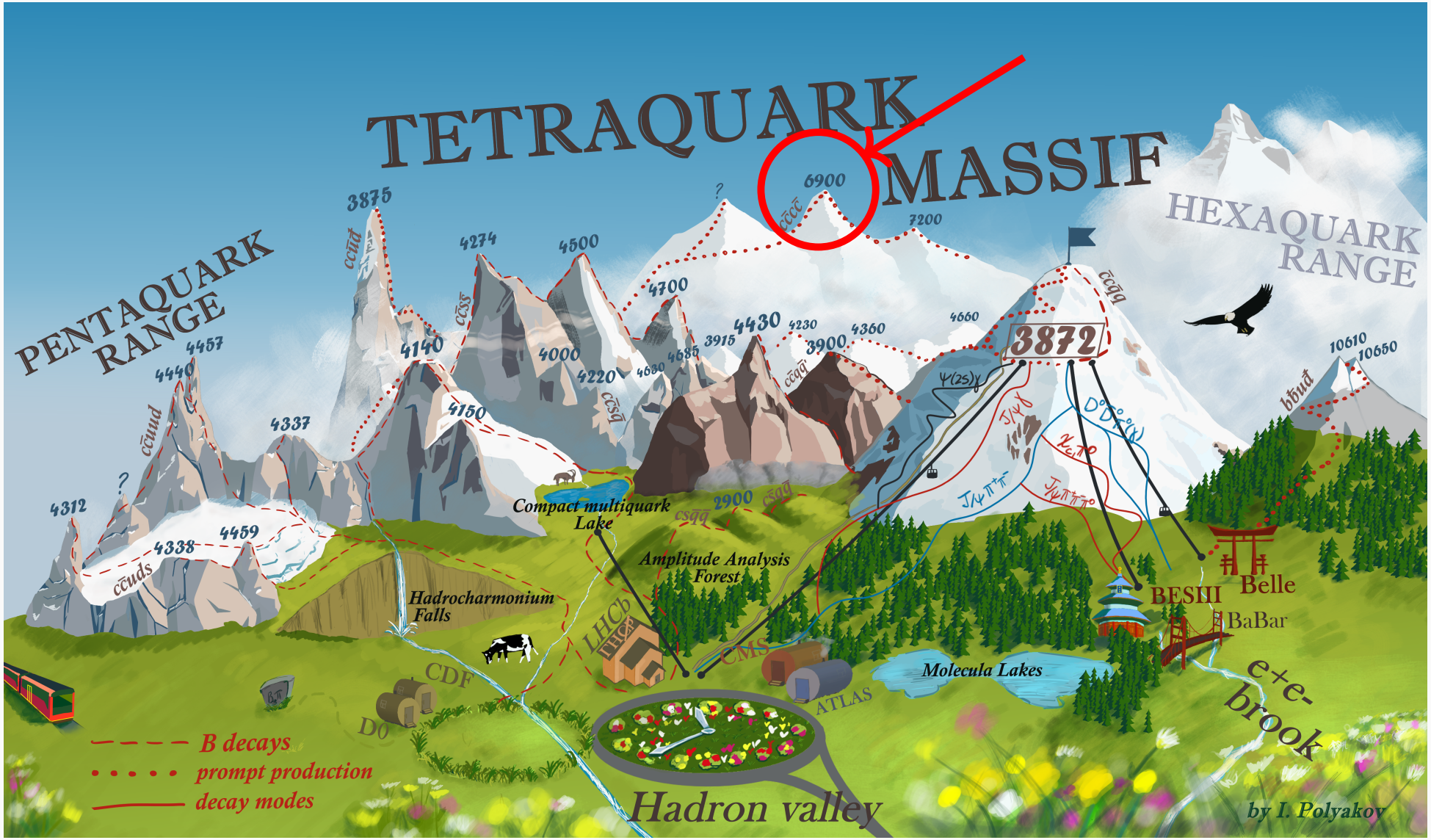

Hüsken et al., Mod.Phys.Lett.A 40 17n18, 2530002 (2025)

$X(6900)$ possible $cc\bar{c}\bar{c}$ tetraquark candidate

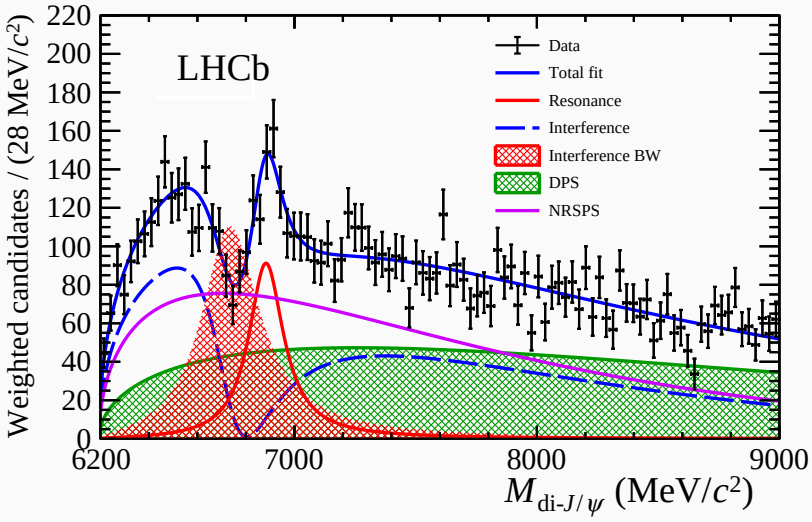

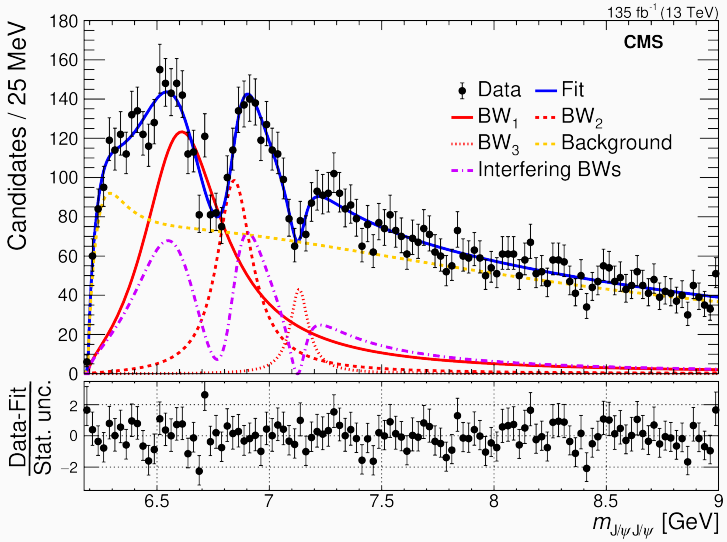

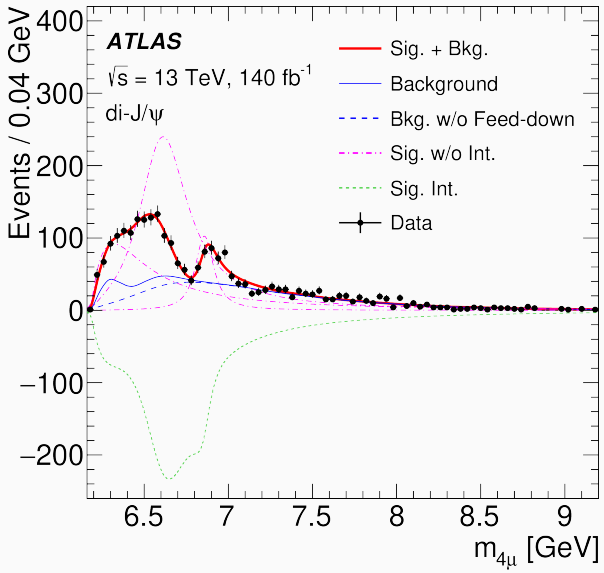

- LHCb observed a narrow structure near $6.9\ \text{GeV}$ in the di-J/ψ spectrum **LHCb, Sci. Bull. 65, 1983 (2020)**
- CMS and ATLAS later confirmed similar structures

  CMS, PRL 132, 111901 (2024); ATLAS, PRL 131, 151902 (2023)
- A compact $cc\bar{c}\bar{c}$ tetraquark is natural, but threshold and coupled-channel interpretations remain viable.

CMS NAILING J^{PC} FOR $X(6900)$ CMS, Nature 648, 58 (2025)

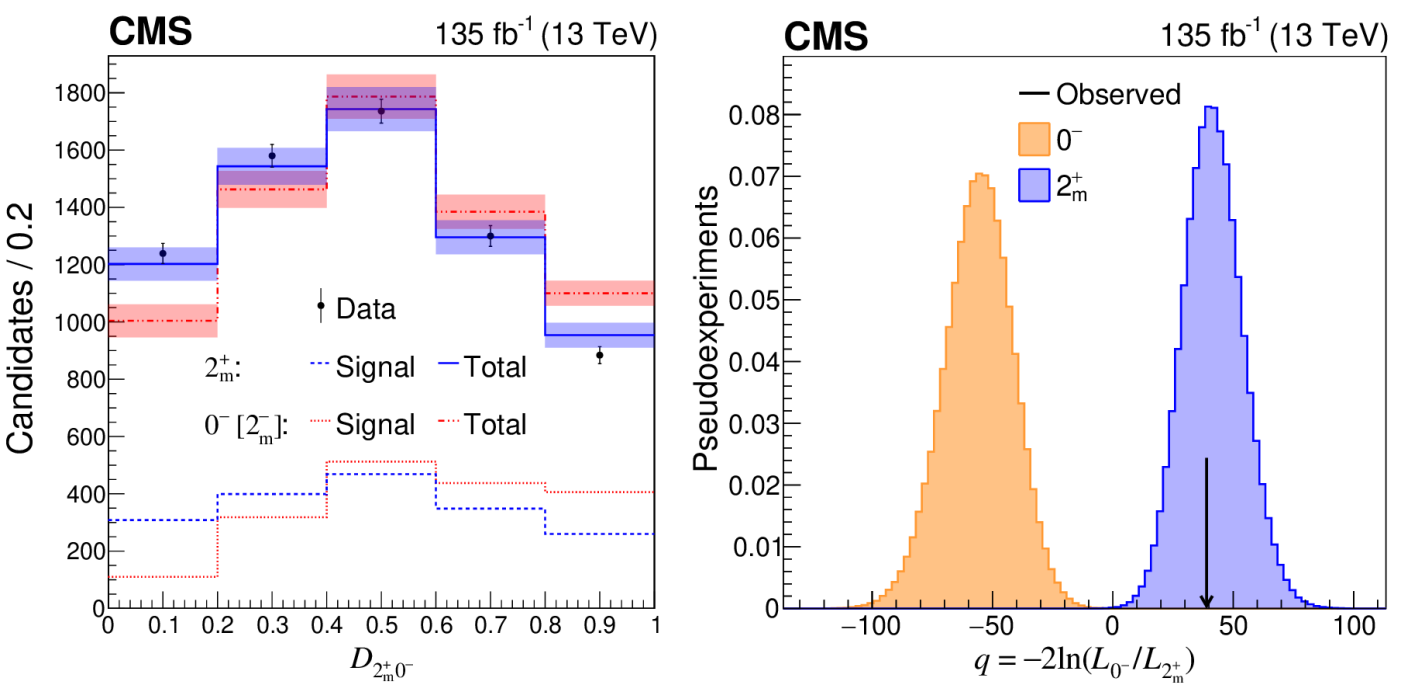

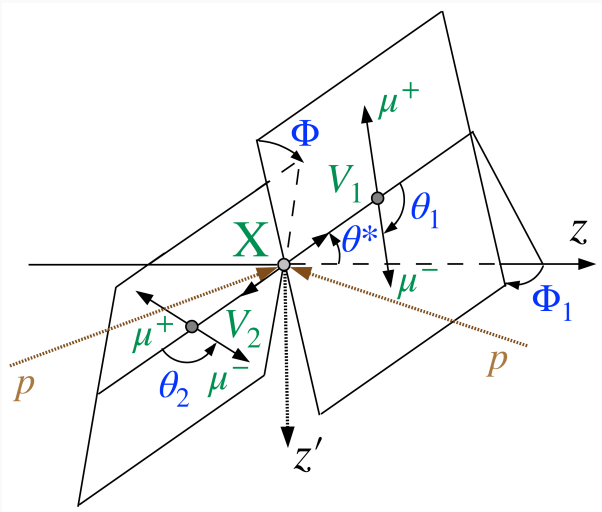

- the quantum numbers are inferred from the J/ψ polarizations, which produce specific angular distributions of the decay muons
- their result favors $J^{PC} = 2^{++}$.

THEORY DEVELOPMENT mass spectra and decays

- Early studies dated back to 70's, mass spectra and decay branching ratios were computed

  Iwasaki, PRL 36, 1266 (1976); Chao, Z. Phys. C 7, 317 (1981)

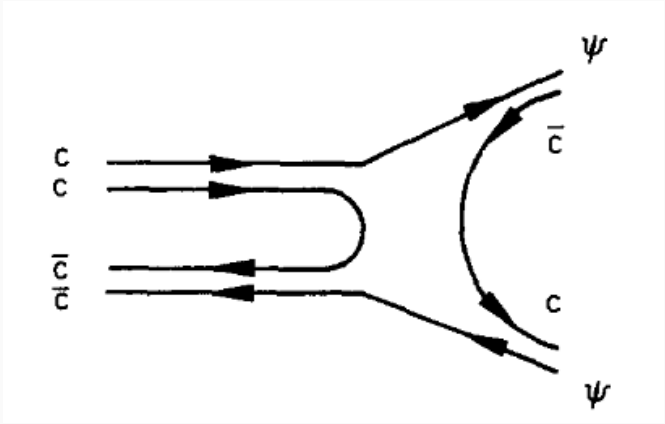

THEORY DEVELOPMENT mass spectra and decays

- Early studies dated back to 70's, mass spectra and decay branching ratios were computed

  Iwasaki, PRL 36, 1266 (1976); Chao, Z. Phys. C 7, 317 (1981)

- Many potential models and QCD sum rules studies followed, with extensive mass spectra and decay predictions
- lattice QCD calculation: no $bb\bar{b}\bar{b}$ bound state

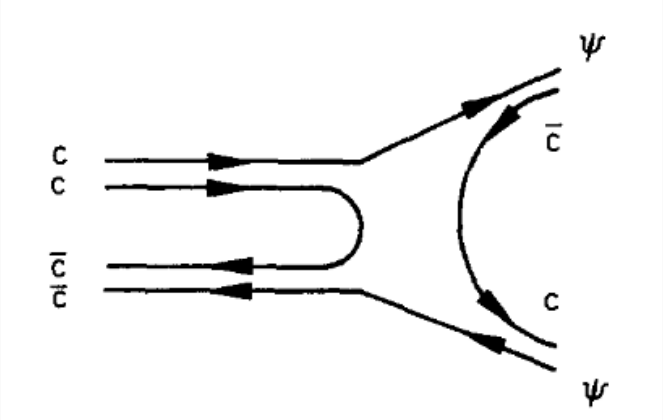

THEORY DEVELOPMENT mass spectra and decays

- Early studies dated back to 70's, mass spectra and decay branching ratios were computed

  Iwasaki, PRL 36, 1266 (1976); Chao, Z. Phys. C 7, 317 (1981)

- Many potential models and QCD sum rules studies followed, with extensive mass spectra and decay predictions
- lattice QCD calculation: no $bb\bar{b}\bar{b}$ bound state
- potential NRQCD calculation concludes no bound $cc\bar{c}\bar{c}$ state, only bound state for unequal-mass scenarios

  Assi & Wagman, 2311.01498v3 (not the published ver.)

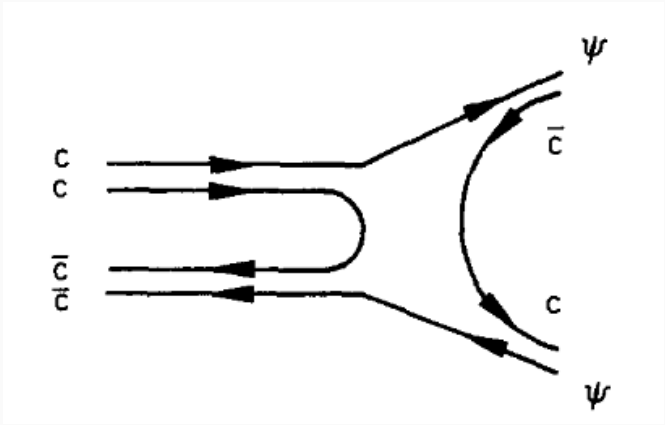

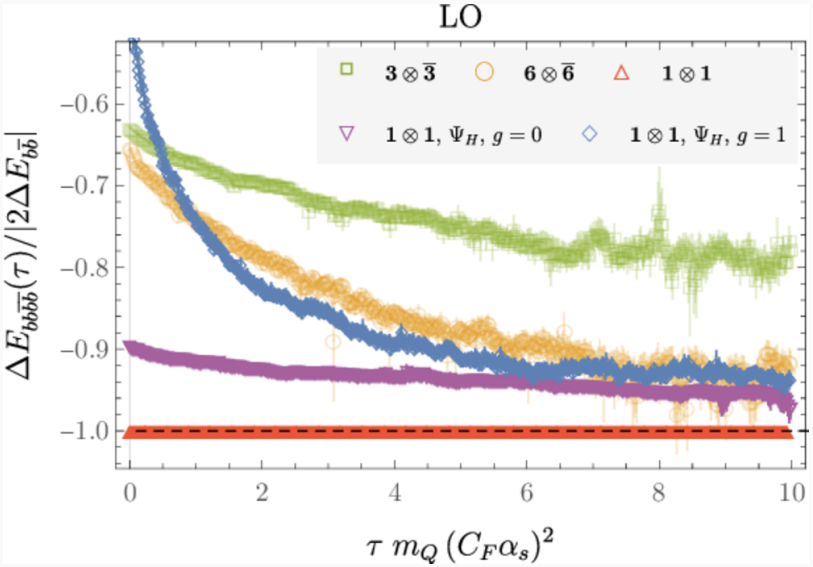

Assi & Wagman, 2311.01498v3.

Below the dash line indicates bound states.

Production of fully-heavy tetraquarks

Predominant method for estimating the production of fully-heavy tetraquarks since 2011 has been the duality or color evaporation model (CEM) approach.

Duality/CEM

summing over all possible hadron final states $\rightarrow$ perturbative partonic calculation

Idea

Integrate an inclusive four-heavy-quark spectrum in a mass window, then multiply by a pheno parameter F_T

$$d\sigma_T = F_T \int_{\Delta M_T} dM_{4Q}\, d\sigma_{4Q}(M_{4Q}).$$

Caveats

- very hand-waving determination of F_H;
- σ_{4Q} usually not computed, but estimated from J/ψ cross sections;
- not properly formulated

Berezhnoy et al., PRD 84, 094023 (2011); Maciula, Schafer & Szczurek, PLB 812, 136010 (2021); ...

CEM IN QUARKONIUM PHYSICS

- CEM has been applied to the production of quarkonia

  see Bodwin, Braaten & Lee, PRD 72, 014004 (2005) for a comparison w/ NRQCD

- Applications to quarkonium production in small-x w/ CGC Watanabe & Xiao, PRD 92, 111502 (2015)
- Its basic mass-window formula is

$$\sigma_{\rm CEM}[AB \to H + X] = F_H \int_{4m^2}^{4m_M^2} dm^2_{Q\bar{Q}} \, \frac{d\sigma}{dm^2_{Q\bar{Q}}}[AB \to Q\bar{Q} + X].$$

- M is the lightest open-flavor meson containing the heavy quark Q (e.g. D meson). $Q\bar{Q}$ pair will hadronize into quarkonium H only with $m_{Q\bar{Q}} < 2m_M$.
- F_H is assumed to be universal, but in the view of NRQCD, it implies relations btw. different NRQCD LDMEs
- no spin information in the spin-summed version

Fritzsch, PLB 67, 217 (1977); Halzen, PLB 69, 105 (1977)

PRODUCTION IN A MEDIUM coalescence model

- Coalescence model in a medium
- multiply the heavy-quark phase-space densities f_i by the tetraquark Wigner function W_T, which measures the overlap with the bound-state wave function.

The yield is estimated from the overlap integral

$$N_T \sim \int d\Gamma_4 \, f_1 f_2 f_3 f_4 \, W_T(\Gamma_4).$$

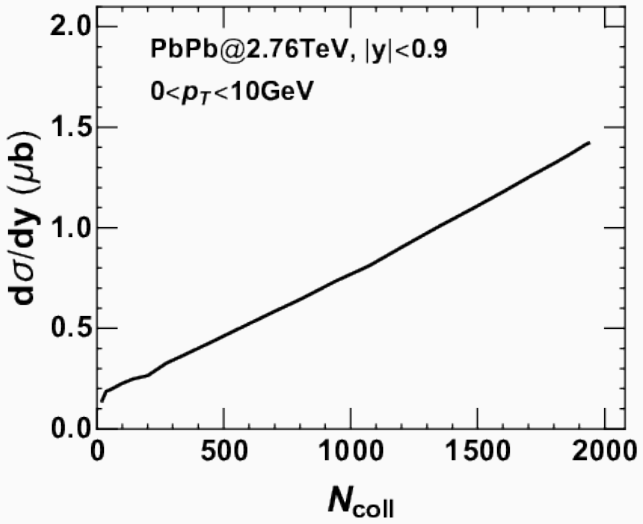

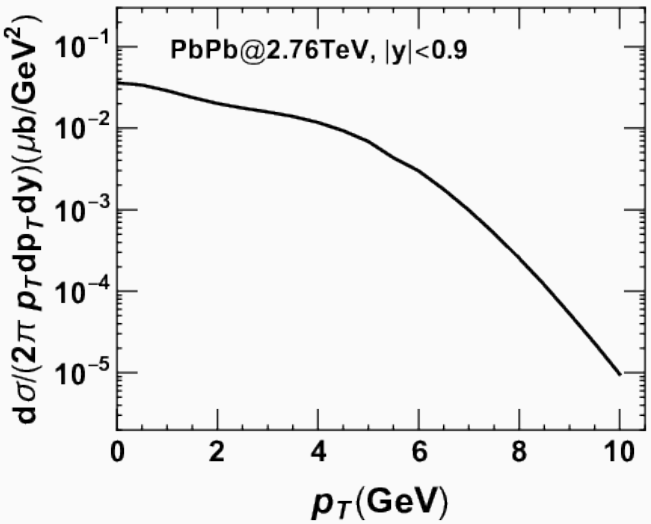

Zhao, Shi & Zhuang, PRD 102, 114001 (2020)

Can we describe T_{4c} production from QCD first principles?

NRQCD Factorization

from quarkonium to T_{4c}

SCALE SEPARATION in quarkonium systems

- Well-separated momentum scales

	$c\bar{c}$	$b\bar{b}$	$t\bar{t}$
m_Q	$1.5\mathrm{GeV}$	$4.7\mathrm{GeV}$	$180\mathrm{GeV}$
$m_Q v$	$0.9\mathrm{GeV}$	$1.5\mathrm{GeV}$	$16\mathrm{GeV}$
$m_Q v^2$	$0.5\mathrm{GeV}$	$0.5\mathrm{GeV}$	$1.5\mathrm{GeV}$
v	0.6	0.3	0.09

	$c\bar{c}$	$b\bar{b}$	$t\bar{t}$
$\alpha_s(m_Q)$	0.35	0.22	0.11
$\alpha_s(m_Q v)$	0.52	0.35	0.16
$\alpha_s\left(m_Q v^2\right)$	$\gg 1$	$\gg 1$	0.35

Braaten, hep-ph/9702225

- $m_Q v$ well within nonperturbative regime ($\sim \Lambda_{\mathrm{QCD}}$) for charm quarks, bottom quarks not far above it
- calls for factorization

NRQCD FACTORIZATION in quarkonium systems

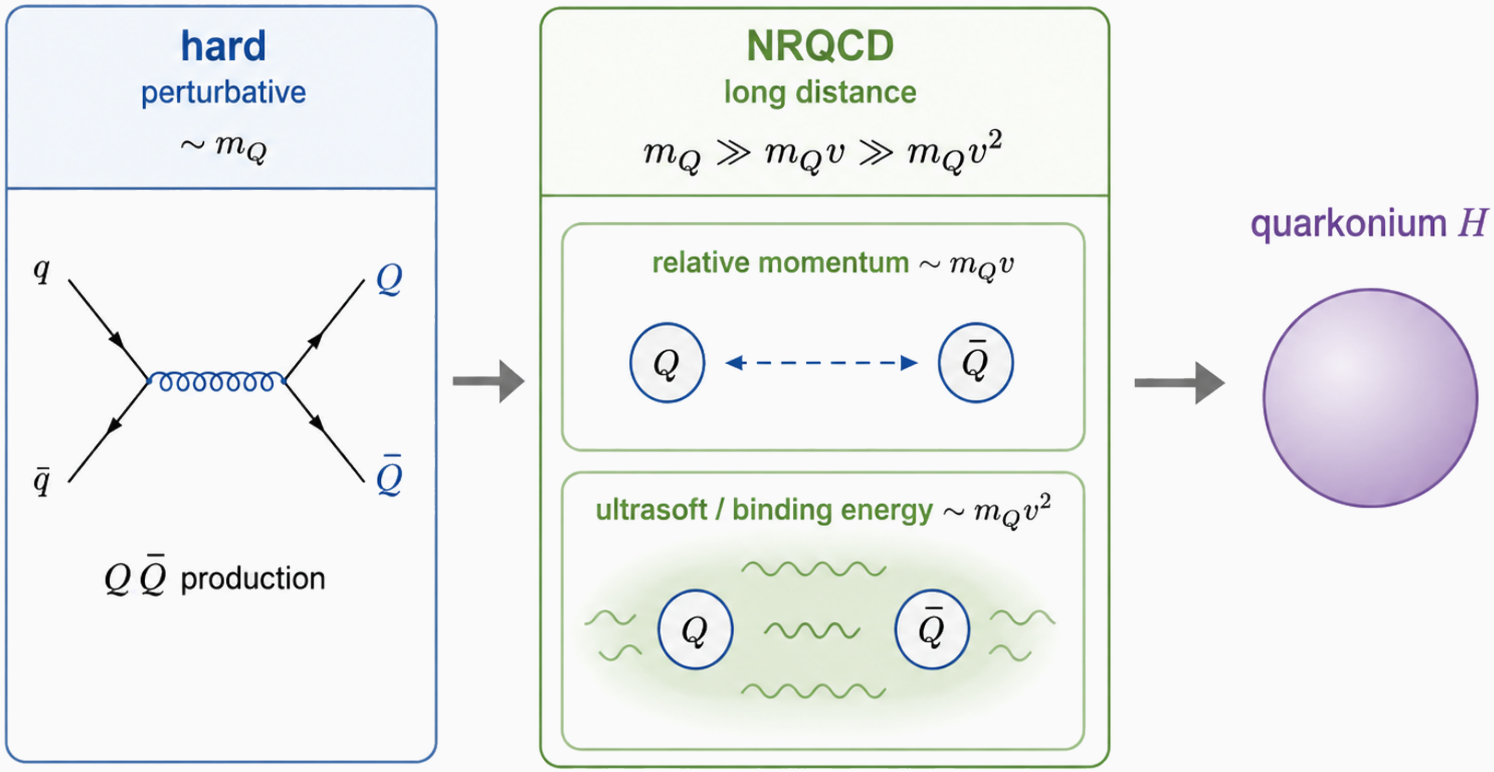

- Factorize the cross section Bodwin, Braaten & Lepage, PRD 51, 1125 (1995)

$$d\sigma(H) = \sum_n F_n(\Lambda)\langle 0|\mathcal{O}_n^H(\Lambda)|0\rangle$$

  - $F_n(\Lambda)$: Short-distance coefficients (SDCs)
  - $\langle 0|\mathcal{O}_n^H(\Lambda)|0\rangle$: Long-distance matrix elements (LDMEs)
  - NRQCD is an EFT w/ velocity power counting, one can add operators $\mathcal{O}_n$ of higher order to improve accuracy

NRQCD factorization formula for $\mathrm{T_{4c}}$ production

$$\mathrm{d}\sigma(T_{4Q}^J + X) = \sum_n F_n^{[J]}(m_c, \mu_\Lambda)\langle 0|\mathcal{O}_n^{T_{4Q},J}(\mu_\Lambda)|0\rangle.$$

SDC $F_n^{[J]}$

$QQ\bar{Q}\bar{Q}$ quarks are produced at short distance ($\sim 1/m_Q$), still well within perturbative regime

LDME $\langle 0|\mathcal{O}_n^{T_{4Q},J}|0\rangle$

Nonperturbative hadronization of the $QQ\bar{Q}\bar{Q}$ system into a physical tetraquark state

S-wave tetraquarks only for this talk

$$J^{PC} = 0^{++}, 1^{+-}, 2^{++}.$$

NRQCD OPERATORS FOR T_{4c} IN DIQUARK BASIS

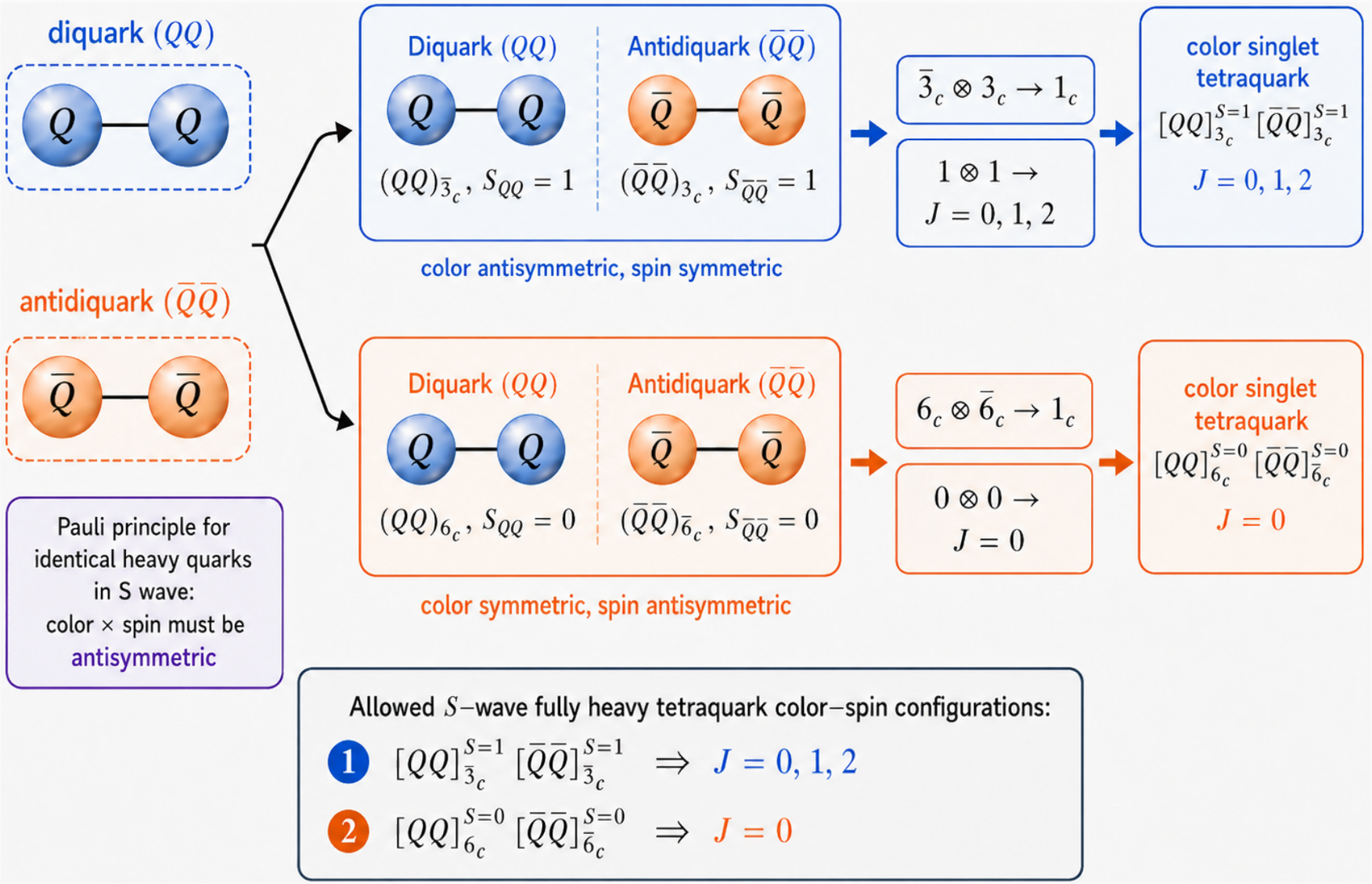

NRQCD OPERATORS FOR T_{4c} IN DIQUARK BASIS

NRQCD production operators for $J^{PC} = 0^{++}, 1^{+-}, 2^{++}$ tetraquarks

$$\mathbb{O}_{3,3}^{(J)} = \mathcal{O}_{\bar{\mathbf{3}}\otimes\mathbf{3}}^{(J)} \sum_X |T_{4c}^J + X\rangle\langle T_{4c}^J + X| \, \mathcal{O}_{\bar{\mathbf{3}}\otimes\mathbf{3}}^{(J)\dagger},$$

$$\mathbb{O}_{6,6}^{(J)} = \mathcal{O}_{\mathbf{6}\otimes\bar{\mathbf{6}}}^{(J)} \sum_X |T_{4c}^J + X\rangle\langle T_{4c}^J + X| \, \mathcal{O}_{\mathbf{6}\otimes\bar{\mathbf{6}}}^{(J)\dagger},$$

$$\mathbb{O}_{3,6}^{(J)} = \mathcal{O}_{\bar{\mathbf{3}}\otimes\mathbf{3}}^{(J)} \sum_X |T_{4c}^J + X\rangle\langle T_{4c}^J + X| \, \mathcal{O}_{\mathbf{6}\otimes\bar{\mathbf{6}}}^{(J)\dagger}.$$

leading-order NRQCD local operators for $J^{PC} = 0^{++}, 1^{+-}, 2^{++}$ states

$$\mathcal{O}_{\bar{\mathbf{3}}\otimes\mathbf{3}}^{(0)} = -\frac{1}{\sqrt{3}}[\psi_a^T(i\sigma^2)\sigma^i\psi_b][\chi_c^\dagger\sigma^i(i\sigma^2)\chi_d^*]\,\mathcal{C}_{\bar{\mathbf{3}}\otimes\mathbf{3}}^{ab;cd},$$ → color projection

$$\mathcal{O}_{\mathbf{6}\otimes\bar{\mathbf{6}}}^{(0)} = [\psi_a^T(i\sigma^2)\psi_b][\chi_c^\dagger(i\sigma^2)\chi_d^*]\,\mathcal{C}_{\mathbf{6}\otimes\bar{\mathbf{6}}}^{ab;cd}, \qquad \mathcal{O}_{\mathbf{6}\otimes\bar{\mathbf{6}}}^{(J>0)} = 0,$$ → only $\mathbb{O}_{3,3}$ for $J = 1, 2$

$$\mathcal{O}_{\bar{\mathbf{3}}\otimes\mathbf{3}}^{i} = \frac{i}{\sqrt{2}}\epsilon^{ijk}[\psi_a^T\sigma^j(i\sigma^2)\psi_b][\chi_c^\dagger(i\sigma^2)\sigma^k\chi_d^*]\,\mathcal{C}_{\bar{\mathbf{3}}\otimes\mathbf{3}}^{ab;cd},$$

$$\mathcal{O}_{\bar{\mathbf{3}}\otimes\mathbf{3}}^{\alpha\beta;(2)} = [\psi_a^T(i\sigma^2)\sigma^m\psi_b][\chi_c^\dagger\sigma^n(i\sigma^2)\chi_d^*]\,\Gamma^{\alpha\beta;mn}\mathcal{C}_{\bar{\mathbf{3}}\otimes\mathbf{3}}^{ab;cd}.$$

Feng, YH, Jia et al., PRD 106, 114029 (2022); YH, Feng, Jia et al., CPC 45, 093101 (2021)

NRQCD production operators for $J^{PC} = 0^{++}, 1^{+-}, 2^{++}$ tetraquarks

Color Projection:

$$\mathcal{C}^{ab;cd}_{\bar{\mathbf{3}}\otimes\mathbf{3}} \equiv \frac{1}{(\sqrt{2})^2}\epsilon^{abm}\epsilon^{cdn}\frac{\delta^{mn}}{\sqrt{3}} = \frac{1}{2\sqrt{3}}(\delta^{ac}\delta^{bd} - \delta^{ad}\delta^{bc})$$

$$\mathcal{C}^{ab;cd}_{\mathbf{6}\otimes\bar{\mathbf{6}}} \equiv \frac{1}{2\sqrt{6}}(\delta^{ac}\delta^{bd} + \delta^{ad}\delta^{bc}).$$

$$\Gamma^{kl;mn} \equiv \frac{1}{2}(\delta^{km}\delta^{ln} + \delta^{kn}\delta^{lm} - \frac{2}{3}\delta^{kl}\delta^{mn})$$

Vacuum-saturation approximation (VSA): drop summation over X in the state projection $\mathcal{P} = \sum_X |T_{4c}(P)+X\rangle\langle T_{4c}(P)+X|$

$$\langle 0|\mathcal{O}|0\rangle \to \sum_X \left\langle 0\middle|\mathcal{O}^{(J)}_{\rm color}\middle|T^{(J)}_{4c}+X\right\rangle \left\langle T^{(J)}_{4c}+X\middle|\mathcal{O}^{(J)\dagger}_{\rm color}\middle|0\right\rangle$$

$$\to \left|\left\langle 0\middle|\mathcal{O}^{(J)}_{\rm color}\middle|T^{(J)}_{4c}\right\rangle\right|^2$$

leading-orc

ojection

→ only $\mathcal{O}_{3,3}$ for $J = 1, 2$

$$\mathcal{O}^{\alpha\beta;(2)}_{\bar{\mathbf{3}}\otimes\mathbf{3}} = [\psi^T_a(i\sigma^2)\sigma^m\psi_b][\chi^\dagger_c\sigma^n(i\sigma^2)\chi^*_d]\,\Gamma^{\alpha\beta;mn}\mathcal{C}^{ab;cd}_{\bar{\mathbf{3}}\otimes\mathbf{3}}.$$

Feng, YH, Jia et al., PRD 106, 114029 (2022); YH, Feng, Jia et al., CPC 45, 093101 (2021)

SDCs are not sensitive to IR physics, so they can be determined by perturbative matching.

1. Replace the physical tetraquark by a free $cc\bar{c}\bar{c}$ state carrying the same color and spin quantum numbers.

$$\left|T_{4c}^{J}\right\rangle \to \left|[QQ\bar{Q}\bar{Q}]^{(J)}\right\rangle$$

2. Compute the cross section on the QCD side and the NRQCD operator matrix elements on the EFT side **perturbatively**.
3. Solve the matching relation for the SDCs F_n.

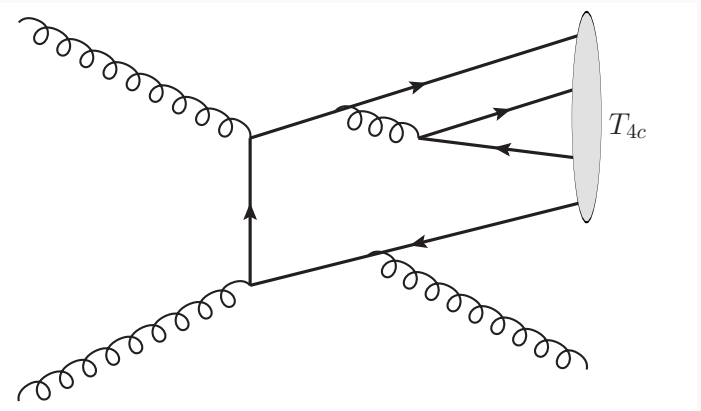

Typical perturbative diagram entering the matching of $pp \to T_{4c} + X$

Perturbative matching statement

$$\mathrm{d}\sigma([\mathbf{QQ\bar{Q}\bar{Q}}]^{\mathbf{J}} + X) = \sum_n F_n^{[J]}(m_c, \mu_\Lambda)\langle 0|\mathcal{O}_n^{[\mathbf{QQ\bar{Q}\bar{Q}}],J}(\mu_\Lambda)|0\rangle.$$

Here NRQCD local matrix elements $\left\langle 0\middle|\mathcal{O}\middle|[\mathbf{QQ\bar{Q}\bar{Q}}]^{\mathbf{J}}\right\rangle$ are all normalized to 4.

- Amplitude calculation with Clebsch-Gordan coefficients in the angular momentum eigenstates: use covariant projectors
- Standard technique for quarkonium production/decay
- Two spinors are projected into spin-0/1 diquark state with projector Π

$$\sum_{\lambda_1,\lambda_2} v\left(-\mathbf{p},\lambda_1\right)\bar{u}\left(\mathbf{p},\lambda_2\right)\left\langle \frac{1}{2}\lambda_1\frac{1}{2}\lambda_2\middle|Ss_z\right\rangle \to \Pi_S$$

Spin-$1/2$ projectors Π

$$\Pi_0 = \frac{1}{4\sqrt{2}m}\gamma^5(\not{P}+2m)$$
$$\Pi_1^\mu = \frac{1}{4\sqrt{2}m}\gamma^\mu(\not{P}+2m)$$

- Use charge conjugation operator C to convert $v \leftrightarrow \bar{u}$

- Clebsch-Gordan coefficients between two spin-1 polarization vectors are represented by $J^{\mu\nu}$ (similar to projectors for spin-orbital coupling)

Spin-1 projectors $J^{\mu\nu}$

$$\eta^{\mu\nu}(p) = -g^{\mu\nu} + \frac{p^\mu p^\nu}{p^2}$$

$$J_0^{\mu\nu} = \frac{1}{\sqrt{3}}\eta^{\mu\nu}(p)$$

$$J_1^{\mu\nu}(\epsilon) = -\frac{i}{\sqrt{2p^2}}\varepsilon^{\mu\nu\rho\sigma}\epsilon_\rho p_\sigma$$

$$J_2^{\mu\nu}(\epsilon) = \epsilon_{\rho\sigma}\left\{\frac{1}{2}\left[\eta^{\mu\rho}(p)\eta^{\nu\sigma}(p) + \eta^{\mu\sigma}(p)\eta^{\nu\rho}(p)\right] - \frac{1}{3}\eta^{\mu\nu}(p)\eta^{\rho\sigma}(p)\right\}$$

- Rules for substitution:

$$\bar{u}_i^a \bar{u}_j^b v_k^c v_l^d \to (\mathrm{C}\Pi_\mu)^{ij}(\Pi_\nu \mathrm{C})^{lk} \mathcal{C}_{\text{color}}^{ab;cd} J_{0,1,2}^{\mu\nu}.$$

where $\mathrm{C} \equiv i\gamma^2\gamma^0$ is the charge conjugation matrix

- NRQCD LDMEs are nonperturbative quantities and ultimately need lattice input or extraction from data.
- In this talk we use potential models to estimate the LDMEs.
  - LDMEs in terms of wave functions at the origin:

$$\langle O^{(0)}_{C_1,C_2}\rangle \approx 16\,\psi^{(0)}_{C_1}(0)\,\psi^{(0)*}_{C_2}(0),$$
$$\langle O^{(1)}_{C_1,C_2}\rangle \approx 48\,\psi^{(1)}_{C_1}(0)\,\psi^{(1)*}_{C_2}(0),$$
$$\langle O^{(2)}_{C_1,C_2}\rangle \approx 80\,\psi^{(2)}_{C_1}(0)\,\psi^{(2)*}_{C_2}(0).$$

- $\psi(0)$ denotes the four-body Schrödinger wave function at the origin.
- The color labels C_1 and C_2 can be either 3 or 6, corresponding to the $\bar{\mathbf{3}}\otimes\mathbf{3}$ and $\mathbf{6}\otimes\bar{\mathbf{6}}$ diquark-antidiquark channels.
- **SDCs are robust; LDME values are not.**
  LDMEs are the main source of uncertainty in the phenomenological predictions.

Phenomenological Applications

LHC, Belle II, and EIC

Fragmentation production of T_{4c} @LHC

Leading-power QCD factorization at high p_T

$$\mathrm{d}\sigma[pp \to T_{4c} + X] = \sum_i f_{a/p} \otimes f_{b/p} \otimes \mathrm{d}\hat{\sigma}[ab \to i + X] \otimes D_{i \to T_{4c}} + \mathcal{O}(1/p_T).$$

- Fragmentation function (FF) $D_{i \to H}$ is a non-perturbative and process-independent quantity describing the probability of parton i fragments into hadron H.
- Collins and Soper gave their definition of FF in 1981 **Collins & Soper, NPB 194, 445 (1982)**

Collins-Soper definition of $g \to T_{4c}$ fragmentation function

$$D_{g \to T_{4c}}(z, \mu) = \frac{-g_{\mu\nu} z^{d-3}}{2\pi k^+ \left(N_c^2 - 1\right)(d-2)} \int_{-\infty}^{+\infty} \mathrm{d}x^- e^{-ik^+ x^-}$$
$$\times \left\langle 0 \left| G_c^{+\mu}(0) \mathcal{E}^\dagger \left(0, 0, \mathbf{0}_\perp\right)_{cb} \mathcal{P}_{T_{4c}(P)} \mathcal{E}\left(0, x^-, \mathbf{0}_\perp\right)_{ba} G_a^{+\nu}\left(0, x^-, \mathbf{0}_\perp\right) \right| 0 \right\rangle$$
$$\mathcal{P}_{T_{4c}(P)} \equiv \sum_X |T_{4c}(P) + X\rangle\langle T_{4c}(P) + X|$$

- $z \equiv P^+/k^+$ is the light-cone momentum fraction
- $\mathcal{E}$ is a gauge link

Fragmentation production of T_{4c} @LHC

Leading-power QCD factorization at high p_T

$$\mathrm{d}\sigma[pp \to T_{4c} + X] = \sum_i f_{a/p} \otimes f_{b/p} \otimes \mathrm{d}\hat{\sigma}[ab \to i + X] \otimes D_{i \to T_{4c}} + \mathcal{O}(1/p_T).$$

- Fragmentation function (FF) $D_{i \to H}$ is a non-perturbative and process-independent quantity describing the probability of parton i fragments into hadron H.
- Collins and Soper gave their definition of FF in 1981 **Collins & Soper, NPB 194, 445 (1982)**

Collins-Soper definition of $q \to T_{4c}$ fragmentation function

$$D_{q \to H}(z, \mu) = \frac{z^{d-3}}{2\pi \times 4 \times N_c} \int_{-\infty}^{+\infty} \mathrm{d}x^- \, e^{-iP^+ x^-/z}$$
$$\times \mathrm{Tr}\left[\hat{n}\langle 0|\Psi(0)\Phi^\dagger(0,0,\mathbf{0}_\perp)\mathcal{P}_{T_{4c}(P)}\Phi(0,x^-,\mathbf{0}_\perp)\bar{\Psi}(0,x^-,\mathbf{0}_\perp)|0\rangle\right],$$
$$\mathcal{P}_{T_{4c}(P)} \equiv \sum_X |T_{4c}(P) + X\rangle\langle T_{4c}(P) + X|$$

- $z \equiv P^+/k^+$ is the light-cone momentum fraction
- $\mathcal{E}$ is a gauge link

Evolution of fragmentation functions

The fragmentation function $D_{i\to T_{4c}}$ follows the DGLAP evolution equation

$$\mu\frac{\partial}{\partial\mu}D_{i\to T_{4c}}(z,\mu)=\frac{\alpha_s}{\pi}\sum_{j\in\{q,g\}}\int_z^1\frac{\mathrm{d}y}{y}P_{ji}\left(\frac{z}{y},\mu\right)D_{j\to T_{4c}}(y,\mu).$$

LO splitting functions

$$\begin{aligned}
P_{qq}(z)&=C_F\left[\frac{1+z^2}{(1-z)_+}+\frac{3}{2}\delta(1-z)\right],\\
P_{gq}(z)&=C_F\frac{1+(1-z)^2}{z},\\
P_{qg}(z)&=T_F\left[z^2+(1-z)^2\right],\\
P_{gg}(z)&=2C_A\left[\frac{1-z}{z}+\frac{z}{(1-z)_+}+z(1-z)\right]+\frac{\beta_0}{2}\delta(1-z).
\end{aligned}$$

$$C_F=\tfrac{4}{3},T_F=\tfrac{1}{2},C_A=3,\beta_0=11-\tfrac{2}{3}n_f.$$

DGLAP equations are numerically solved to evolve the FFs from the initial scale $\mu_0\sim 4m_c$

NRQCD FACTORIZATION OF FRAGMENTATION FUNCTION

NRQCD factorization for the fragmentation function

$$D_{g\to T_{4c}^J}(z,\mu_\Lambda)=\frac{d_{3,3}^{(J)}(z)}{m_c^9}\langle O_{3,3}^{(J)}\rangle+\frac{d_{6,6}^{(J)}(z)}{m_c^9}\langle O_{6,6}^{(J)}\rangle+\frac{2d_{3,6}^{(J)}(z)}{m_c^9}\,\mathrm{Re}\,\langle O_{3,6}^{(J)}\rangle$$

Representative Feynman diagrams for $g/c/q$ fragmentation channels.

$g \to T_{4c}$

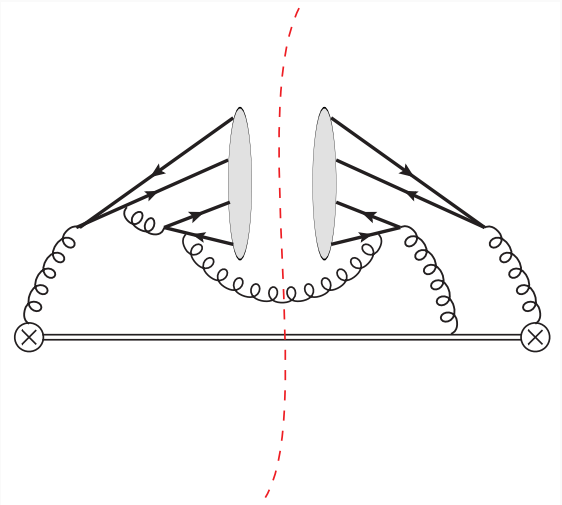

Feng, YH, Jia et al., PRD 106, 114029 (2022)

$c \to T_{4c}$

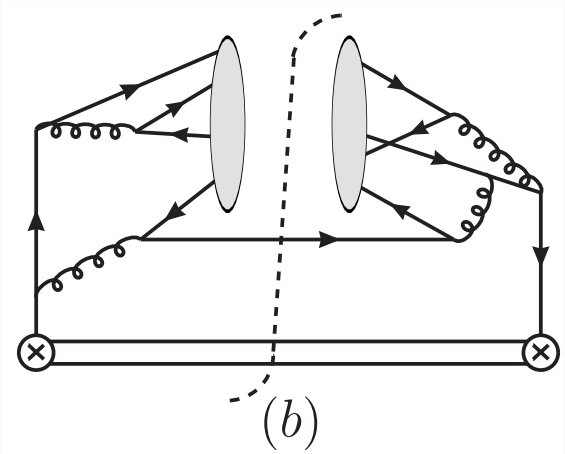

Bai, Feng, YH et al., JHEP 09, 002 (2024)

$q \to T_{4c}$

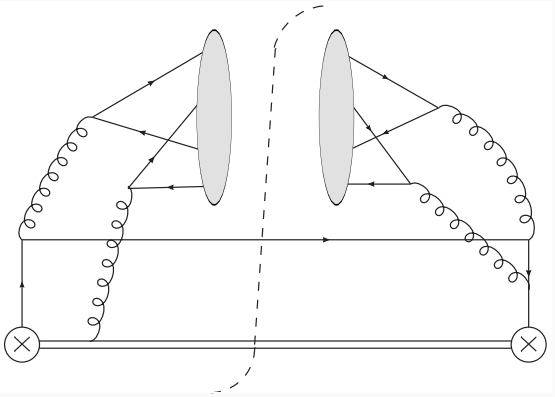

Bai, YH & Sang, PRD 111, 054006 (2025)

Grey blob: physical tetraquark, projected perturbative $|cc\bar{c}\bar{c}\rangle$ in practice

Double line: eikonal gauge link in the fragmentation-function definition.

SDCs FOR $g \to T_{4c}$ Feng, YH, Jia et al., PRD 106, 114029 (2022)

- The short-distance coefficients are determined by perturbative matching: replace the physical tetraquark by a free $cc\bar{c}\bar{c}$ state and match the QCD result onto the NRQCD operator basis.
- For 0^{++}, all three channels $d_{3,3}$, $d_{6,6}$ and $d_{3,6}$ contribute already at leading order.
- For 2^{++}, the leading result is simpler: only the $\bar{\mathbf{3}} \otimes \mathbf{3}$ channel survives.

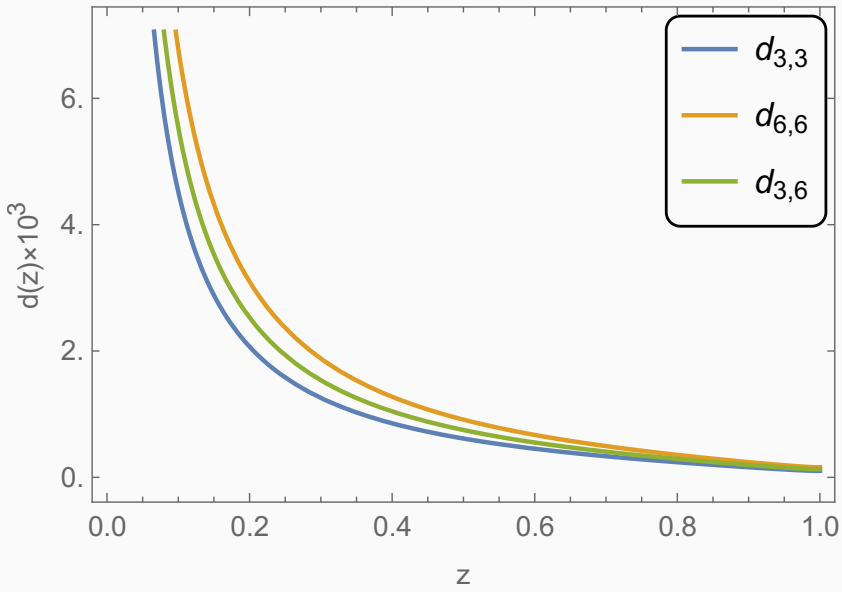

0^{++} SDCs

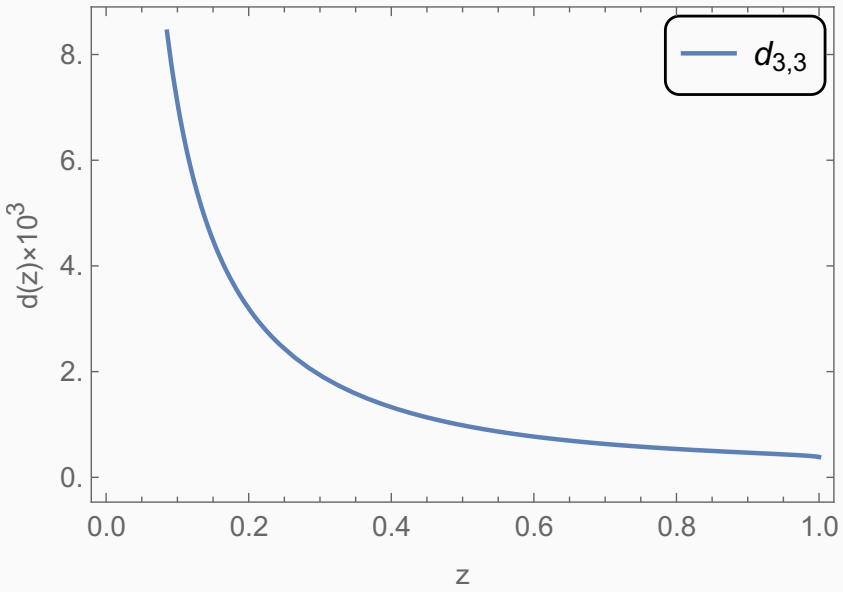

2^{++} SDCs

$$
\begin{aligned}
d_{3,3}\left(g \to 0^{++}\right) =& \frac{\pi^2 \alpha_s^4}{497664 z (2-z)^2 (3-z)} \left[186624 - 430272 z + 511072 z^2 - 425814 z^3 + 217337 z^4\right. \\
& -61915 z^5 + 7466 z^6 + 42 (1-z)(2-z)(3-z)\left(-144 + 634 z - 385 z^2 + 70 z^3\right) \\
& \times \log(1-z) + 36 (2-z)(3-z)\left(144 - 634 z + 749 z^2 - 364 z^3 + 74 z^4\right) \log\left(1 - \frac{z}{2}\right) \\
& \left. +12 (2-z)(3-z)\left(72 - 362 z + 361 z^2 - 136 z^3 + 23 z^4\right) \log\left(1 - \frac{z}{3}\right)\right], \\
d_{6,6}\left(g \to 0^{++}\right) =& \frac{\pi^2 \alpha_s^4}{331776 z (2-z)^2 (3-z)} \left[186624 - 430272 z + 617824 z^2 - 634902 z^3 + 374489 z^4\right. \\
& - 115387 z^5 + 14378 z^6 - 6 (1-z)(2-z)(3-z)\left(-144 - 2166 z + 1015 z^2 + 70 z^3\right) \\
& \times \log(1-z) - 156 (2-z)(3-z)\left(144 - 1242 z + 1693 z^2 - 876 z^3 + 170 z^4\right) \log\left(1 - \frac{z}{2}\right) \\
& \left. +300 (2-z)(3-z)\left(72 - 714 z + 953 z^2 - 472 z^3 + 87 z^4\right) \log\left(1 - \frac{z}{3}\right)\right], \\
d_{3,6}\left(g \to 0^{++}\right) =& \frac{\pi^2 \alpha_s^4}{165888 \sqrt{6} z (2-z)^2 (3-z)} \left[186624 - 430272 z + 490720 z^2 - 394422 z^3 + 199529 z^4\right. \\
& -57547 z^5 + 7082 z^6 + 6 (1-z)(2-z)(3-z)\left(-432 + 3302 z - 1855 z^2 + 210 z^3\right) \\
& \times \log(1-z) - 12 (2-z)(3-z)\left(720 - 2258 z + 2329 z^2 - 1052 z^3 + 226 z^4\right) \log\left(1 - \frac{z}{2}\right) \\
& \left. +12 (2-z)(3-z)\left(936 - 4882 z + 4989 z^2 - 1936 z^3 + 331 z^4\right) \log\left(1 - \frac{z}{3}\right)\right].
\end{aligned}
$$

$$
\begin{aligned}
d_{3,3}\left(g \to 2^{++}\right) =& \frac{\pi^2 \alpha_s^4}{622080 z^2 (2-z)^2 (3-z)} \Big[2 \left(46656 - 490536 z + 1162552 z^2 \right. \\
& \left. -1156308 z^3 + 595421 z^4 - 170578 z^5 + 21212 z^6\right) z \\
& + 3(1-z)(2-z)(3-z)(-20304 - 31788 z) \left(1296 + 1044 z \right. \\
& \left. + 73036 z^2 - 36574 z^3 + 7975 z^4\right) \log(1-z) + 33(2-z)(3-z) \\
& \times \left(1296 + 25 - 9224 z^2 + 9598 z^3 - 3943 z^4 + 725 z^5\right) \log\left(1 - \frac{z}{3}\right)\Big], \\
d_{6,6}\left(g \to 2^{++}\right) =& d_{3,6}\left(g \to 2^{++}\right) = 0.
\end{aligned}
$$

GLUON FRAG. PRODUCTION @LHC

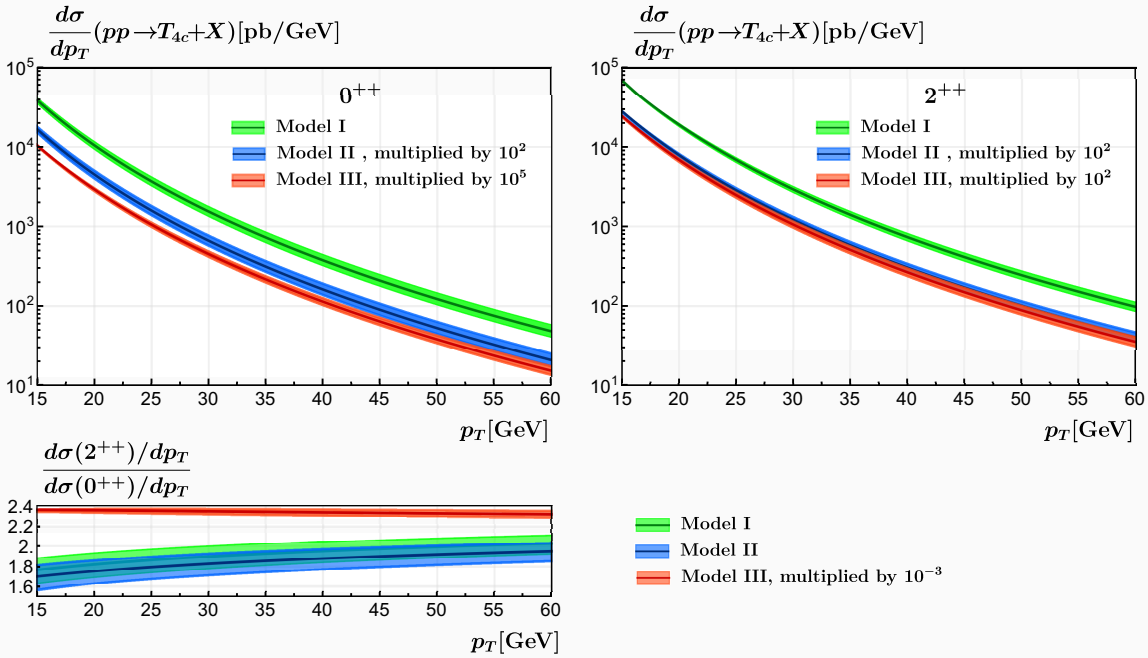

	0^{++}		2^{++}	
Model	σ [pb]	N_{events}	σ [pb]	N_{events}
I	5.5×10^4	1.6×10^{11}	1.0×10^5	3.1×10^{11}
II	2.4×10^2	7.1×10^8	4.3×10^2	1.3×10^9
III	0.16	4.7×10^5	3.7×10^2	1.1×10^9

$$\sqrt{s} = 13\,\text{TeV}, -5 \le y \le 5, 20\,\text{GeV} \le p_T \le 60\,\text{GeV},$$
$$\mathcal{L} = 3000\,\text{fb}^{-1}.$$

- gluon fragmentation is the dominant production channel at high p_T.
- Left fig. shows the p_T spectra with three different LDME models for 0^{++} and 2^{++}.
- The predicted event numbers shown in the table are large, but
  - model I is likely over-optimistic
  - model III has destructive interference in 0^{++}

Feng, YH, Jia et al., PRD 106, 114029 (2022)

OTHER CHANNELS

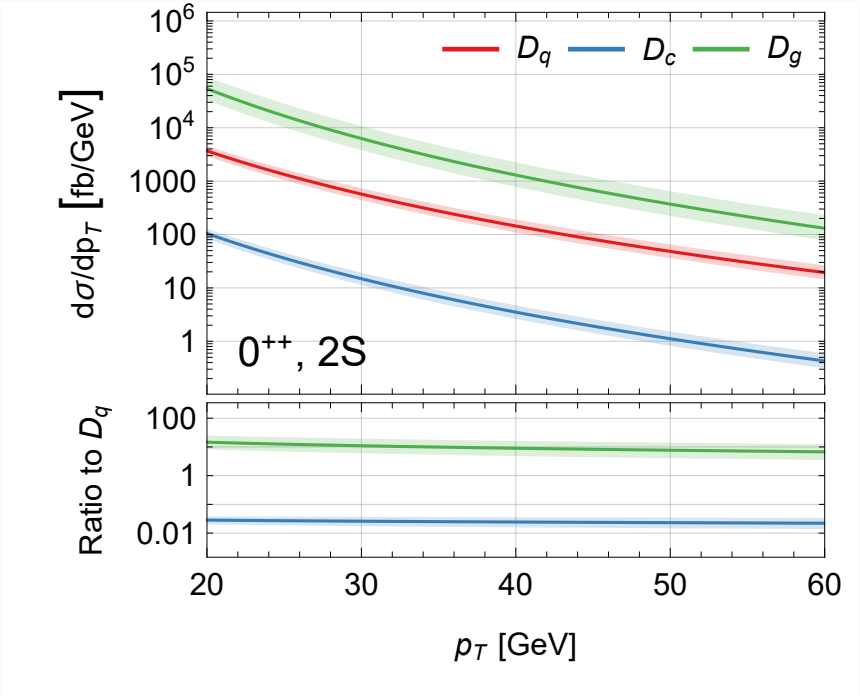

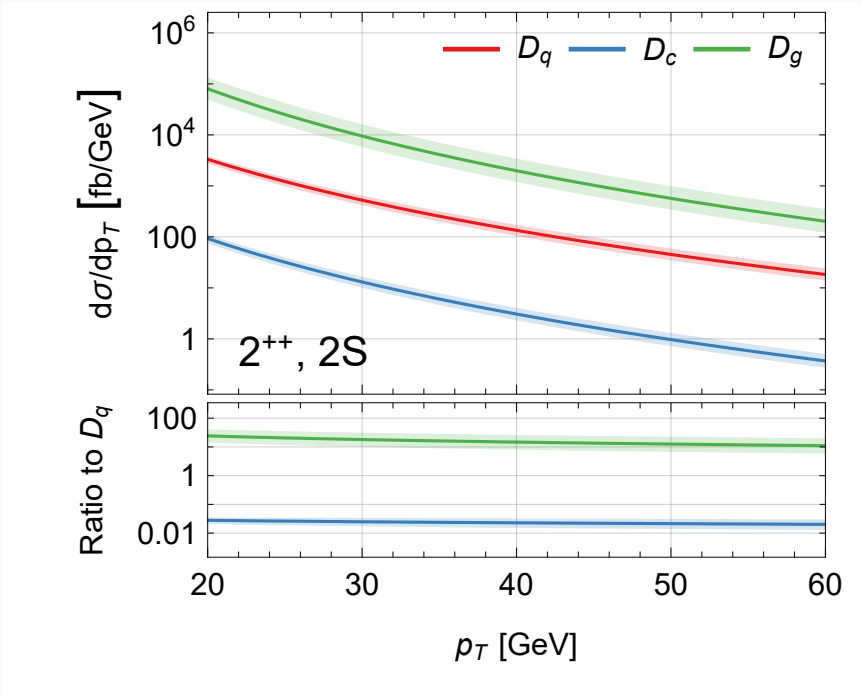

- only model II from previous slide
- light quark channel is approximately one order smaller than gluon channel
- charm quark channel is approximately three orders smaller than gluon channel

Bai, Feng, YH et al., JHEP 09, 002 (2024); Bai, YH & Sang, PRD 111, 054006 (2025)

TetraQuark Fragmentation from NRQCD & symJETHAD

LO

2024 → 2025 → 2026

TQ4Q2.0

Gluon

NEW

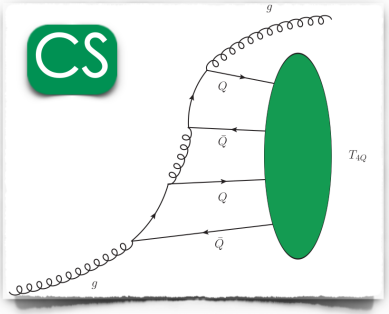

[F. Feng, Y. Huang et al., Phys. Rev. D 106 (2022) 11, 114029]

$J^{PC} = 0^{++}$ TQ4Q1.0+ ✓

$J^{PC} = 1^{+-}$ Landau-Yang LO: evolution only ✗

$J^{PC} = 2^{++}$ TQ4Q1.0+ ✓

Constituent heavy quark

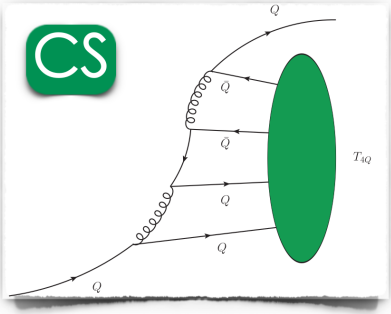

[X.-W. Bai, F. Feng et al., JHEP 09 (2024) 002

TQ4Q1.1+ ✓

TQ4Q1.1+ ✓

TQ4Q1.1+ ✓

Non-constituent heavy or light quark

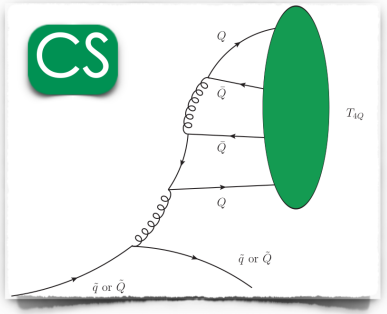

[X.-W. Bai, Y. Huang et al., Phys. Rev. D 111 (2025) 5, 054006]

NEW TQ4Q2.0+ ✓

C-parity LO: evolution only ✗

NEW TQ4Q2.0+ ✓

7

borrowed from Francesco Celiberto's slide at DIS 2026

TQ4Q2.0 vs 1.1?

TetraQuark-Jet Systems with Resummation: Event Yields

Expected events yields [13 TeV Run 2]

T_{4Q}	J^{PC}	TQ4Q2.0	TQ4Q1.1	Δ (%)
T_{4c}	0^{++}	2016031 ± 399168	1768764 ± 309078	+13.98%
T_{4c}	1^{+-}	8619 ± 1770	8619 ± 1612	+0%
T_{4c}	2^{++}	3071882 ± 602910	2721362 ± 480942	+12.88%
T_{4b}	0^{++}	6046 ± 1168	5151 ± 945	+17.38%
T_{4b}	1^{+-}	17 ± 3	17 ± 2	+0%
T_{4b}	2^{++}	8095 ± 1552	7108 ± 828	+13.88%

TABLE IV: Expected event yields for all-b tetraquark production at $\sqrt{s} = 13$ TeV, obtained by integrating the NLL-resummed ΔY distributions in the rapidity range $|\Delta Y| < 6.5$. The yields assume an integrated luminosity of $\mathcal{L}^{(\mathrm{CMS})} = 138.6$ fb^{-1}, corresponding to the total dataset collected by CMS during Run 2 [308, 309]. The last column shows the relative variation $\Delta = (R - 1) \times 100$, with $R =$ TQ4Q2.0/TQ4Q1.1. Uncertainties are propagated from the ΔY distributions and reflect the combined effect of scale variations, FF evolution, and LDME inputs.

Δ(%)

Expected events yields [100 TeV FCC]

T_{4Q}	J^{PC}	TQ4Q2.0	TQ4Q1.1	Δ (%)
T_{4c}	0^{++}	22140238 ± 4433814	19465674 ± 3373524	+13.74%
T_{4c}	1^{+-}	23463 ± 1094	23463 ± 1053	+0%
T_{4c}	2^{++}	32784967 ± 6421338	29144313 ± 5467493	+12.49%
T_{4b}	0^{++}	23424 ± 1982	20237 ± 1552	+15.75%
T_{4b}	1^{+-}	50 ± 2	50 ± 3	+0%
T_{4b}	2^{++}	27894 ± 1972	24493 ± 1323	+13.89%

TABLE V: Expected event yields for all-b tetraquark production at $\sqrt{s} = 100$ TeV, obtained by integrating the NLL-resummed ΔY distributions in the rapidity range $|\Delta Y| < 6.5$. The yields assume an integrated luminosity of $\mathcal{L}^{(\mathrm{CMS})} = 138.6$ fb^{-1}, corresponding to the full Run 2 CMS dataset [308, 309]. This value is conservatively adopted at $\sqrt{s} = 100$ TeV to enable a baseline comparison of energy scaling, independently of specific FCC projections. The last column shows the relative variation $\Delta = (R - 1) \times 100$, with $R =$ TQ4Q2.0/TQ4Q1.1. Uncertainties are propagated from the ΔY distributions and reflect the combined effect of scale variations, FF evolution, and LDME inputs.

Δ(%)

Pile-up effects can degrade Experimental discrimination

4.1 TetraQuark-Jet

16

borrowed from Francesco Celiberto's slide at DIS 2026

Exactly the order of magnitude difference the light quark channel would make!

Low-p_T production at LHC

QCD factorization for fixed order production

$$\mathrm{d}\sigma(pp \to T_{4c} + X) = \sum_{i,j=q,g} \int_0^1 dx_1 dx_2 f_{i/p}(x_1, \mu_F) f_{j/p}(x_2, \mu_F) \times \mathrm{d}\hat{\sigma}_{ij \to T_{4c}+X}(x_1 x_2 s, \mu_F),$$

NRQCD factorization

$$\frac{\mathrm{d}\hat{\sigma}(T_{4c}^{(J)} + X)}{\mathrm{d}\hat{t}} = \frac{2M_{T_{4c}}}{m_c^{14}} \left[F_{3,3}^{(J)} \left\langle O_{3,3}^{(J)} \right\rangle + 2F_{3,6}^{(J)} \left\langle O_{3,6}^{(J)} \right\rangle + F_{6,6}^{(J)} \left\langle O_{6,6}^{(J)} \right\rangle \right],$$

- Fixed-order NRQCD fills low-p_T region where fragmentation don't apply

Feng, YH, Jia et al., PRD 108, L051501 (2023)

LHC fixed-order spectra: Model I

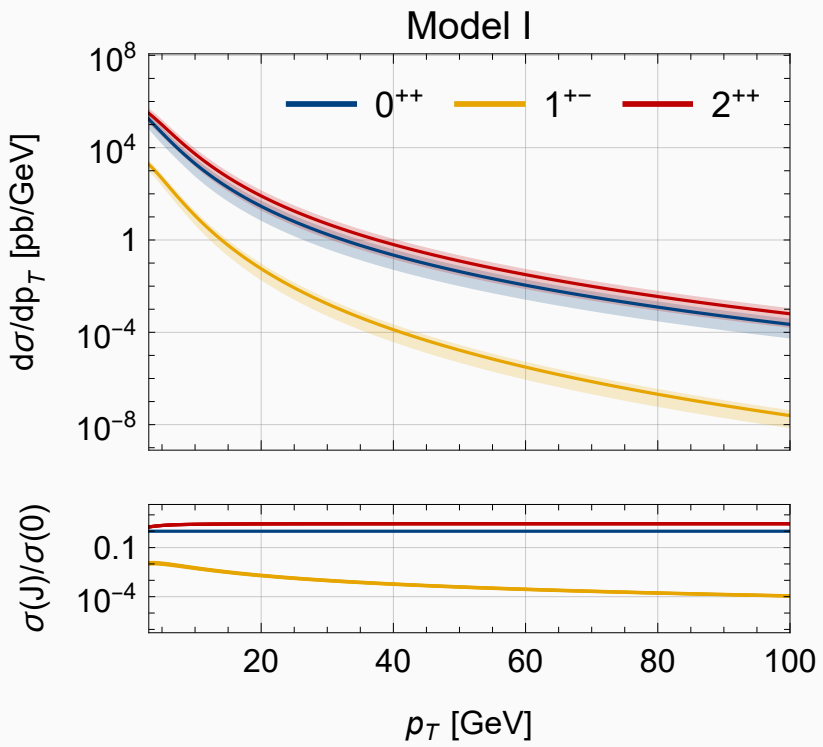

p_T spectra for $J = 0, 1, 2$

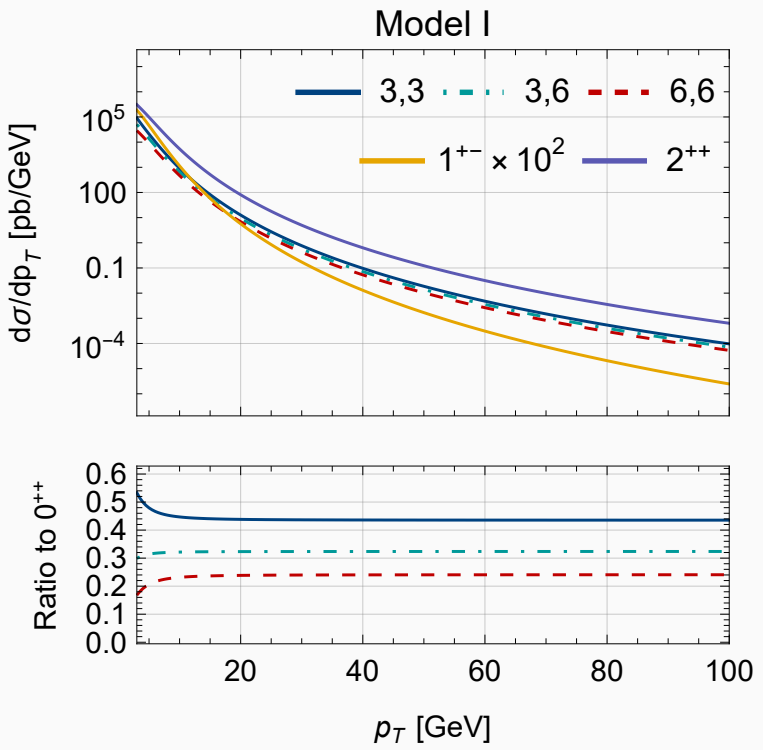

Decomposition of contributions from each color structure

Model I: actually model II in the fragmentation slide

Feng, YH, Jia et al., PRD 108, L051501 (2023)

LHC fixed-order spectra: model II

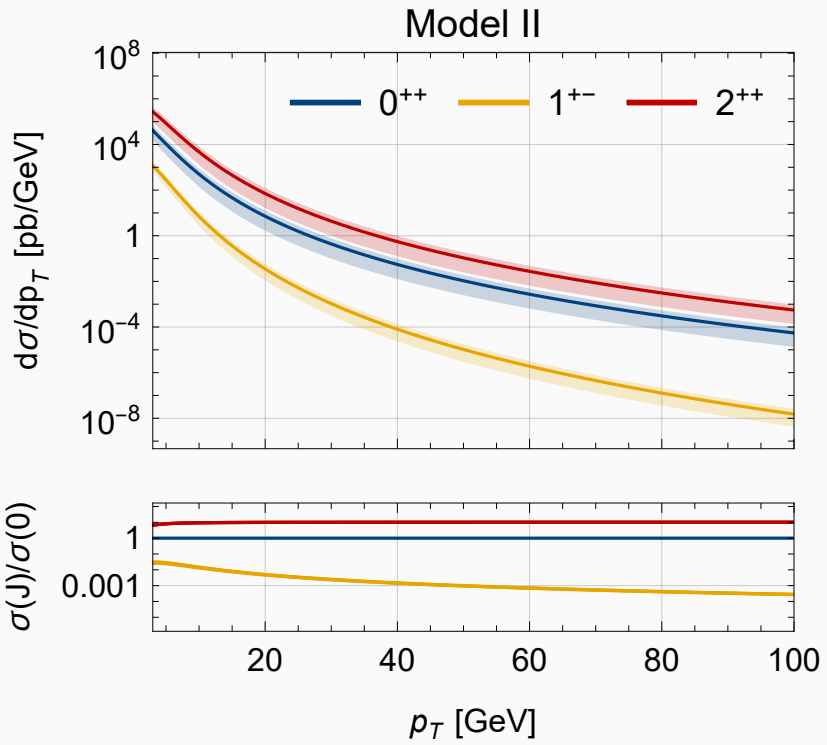

p_T *spectra for* $J = 0, 1, 2$

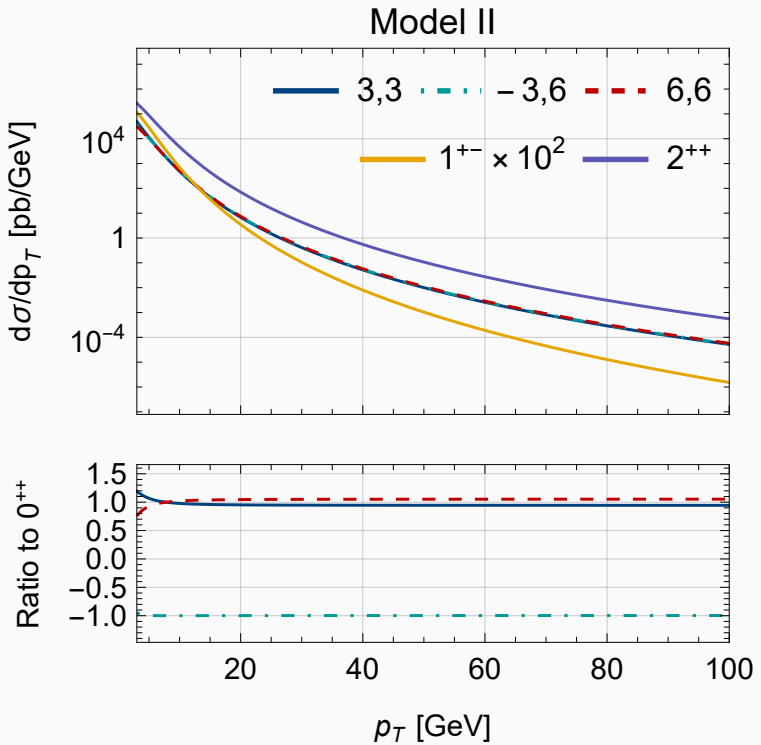

Decomposition of contributions from each color structure

Model II: actually model III in the fragmentation slide, with destructive interference in 0^{++} channel

Feng, YH, Jia et al., PRD 108, L051501 (2023)

LHC: fixed order versus fragmentation

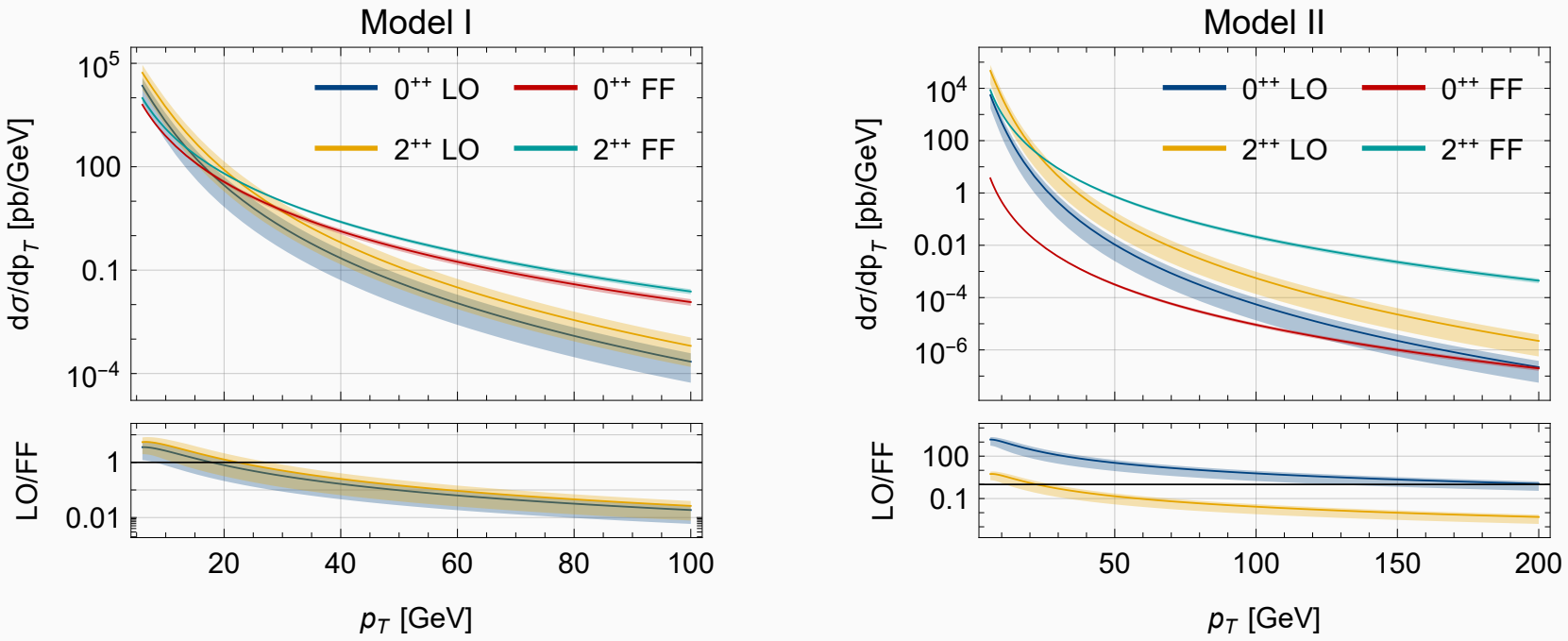

- The leading fixed-order C-even channels scale as p_T^{-6}, while the 1^{+-} channel scales as p_T^{-8}.
- Fragmentation scales as p_T^{-4}, so it gains powers of p_T over fixed-order.
- The crossing around tens of GeV marks where the high-p_T expansion becomes quantitatively preferable.

Feng, YH, Jia et al., PRD 108, L051501 (2023)

Phenomenological Applications

LHC, Belle II, and EIC

Exclusive production at B factory

Feng, YH, Jia et al., PLB 818, 136368 (2021)

NRQCD factorization holds at amplitude level for exclusive process

$$\mathcal{M}^J = \frac{\mathcal{A}^{3[J]}}{m_c^4}\sqrt{2M_{T_{4c}}}\langle T_{4c}^J|\mathcal{O}^{(J)}_{\bar{\mathbf{3}}\otimes\mathbf{3}}|0\rangle + \frac{\mathcal{A}^{6[J]}}{m_c^4}\sqrt{2M_{T_{4c}}}\langle T_{4c}^J|\mathcal{O}^{(J)}_{\mathbf{6}\otimes\bar{\mathbf{6}}}|0\rangle + \mathcal{O}(v^2)$$

Note that here we have the vacuum-to-tetraquark matrix elements $\langle T_{4c}^J|\mathcal{O}^{(J)}_{\mathbf{6}\otimes\bar{\mathbf{6}}}|0\rangle$, not the inclusive ones $\langle O^{(J)}_{6,6}\rangle$.

- For the C-even channels one can study $e^+e^- \to T_{4c}^{0,2} + \gamma$ at Belle II energies.

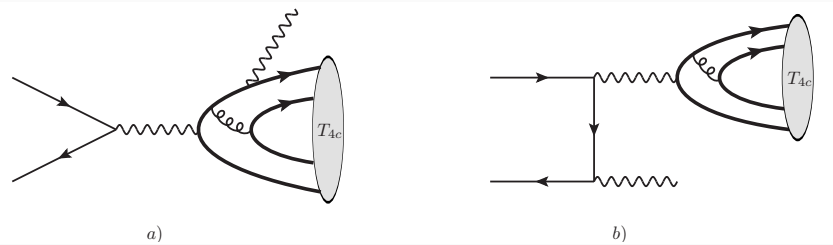

- One can compute the helicity amplitudes to study polarized T_{4c}

$$\frac{\mathrm{d}\sigma\left[e^+e^- \to \gamma\left(\lambda_1\right) + T_{4c}^J\left(\lambda_2\right)\right]}{\mathrm{d}\cos\theta} = \frac{3\alpha}{32\pi s^2}\frac{\left|\mathbf{p}_f\right|}{\sqrt{s}}\left|\mathcal{M}^J_{\lambda_1,\lambda_2}\right|^2 \sum_{S_z=\pm1}\left|d^1_{S_z,\lambda}(\theta)\right|^2 .$$

Belle II: angular distributions

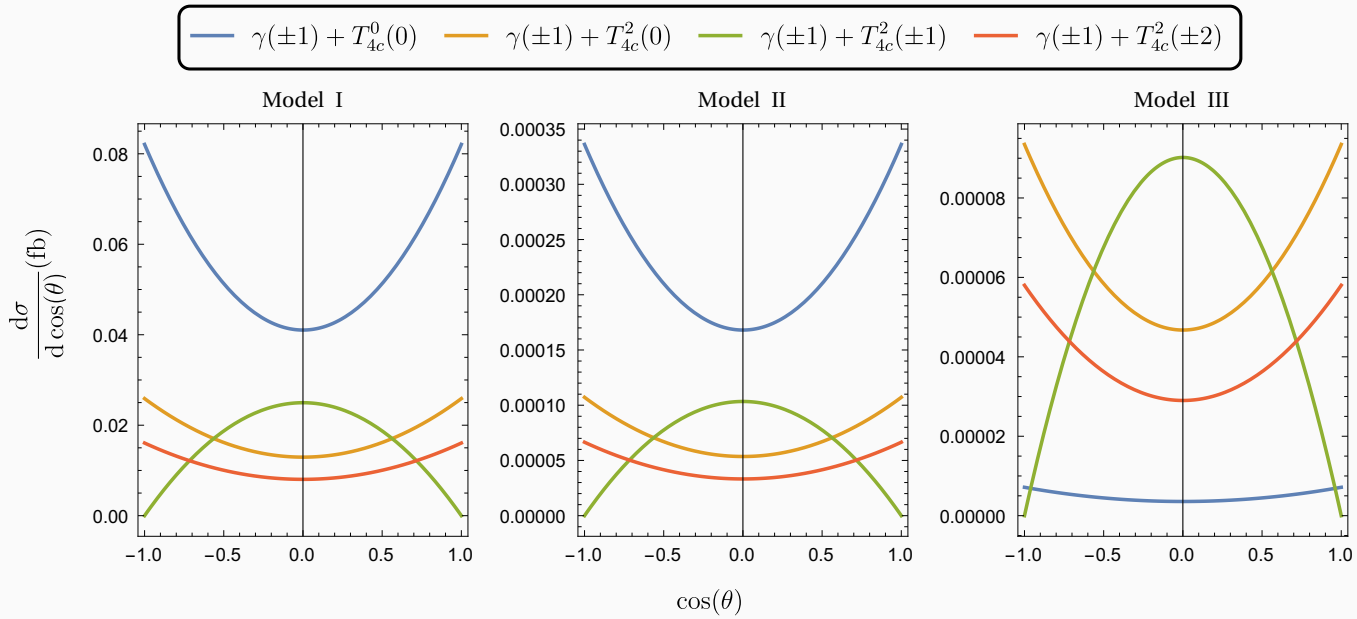

- distinct $T^2_{4c}(\pm1)$ shape, can discern it from T^0_{4c}
- T^0_{4c} more prominent in the forward/backward region

Feng, YH, Jia et al., PLB 818, 136368 (2021)

Production prospects at Belle II

At $\sqrt{s} = 10.58\,\mathrm{GeV}$

$$\sigma(T_{4c}^0 + \gamma) \approx 0.0026\ \mathrm{fb},$$
$$\sigma(T_{4c}^2 + \gamma) \approx 0.020\ \mathrm{fb}.$$

- About 40 s-channel diagrams contribute.
- Before decay and reconstruction losses, Belle II would collect only $\mathcal{O}(10^2)$ $T_{4c}^0 + \gamma$ and $\mathcal{O}(10^3)$ $T_{4c}^2 + \gamma$ events at $50\,\mathrm{ab}^{-1}$.

Compare with ordinary quarkonium

- $e^+e^- \to \eta_c + \gamma$ is about 82 ± 21 fb at the same energy.
- T_{4c} production is much smaller

Feng, YH, Jia et al., PLB 818, 136368 (2021)

BELLE II: INCLUSIVE 1^{+-} CHANNEL YH, Feng, Jia et al., CPC 45, 093101 (2021)

- Access the C-odd channel inclusively:
  $e^+e^- \to T_{4c}(1^{+-}) + gg.$

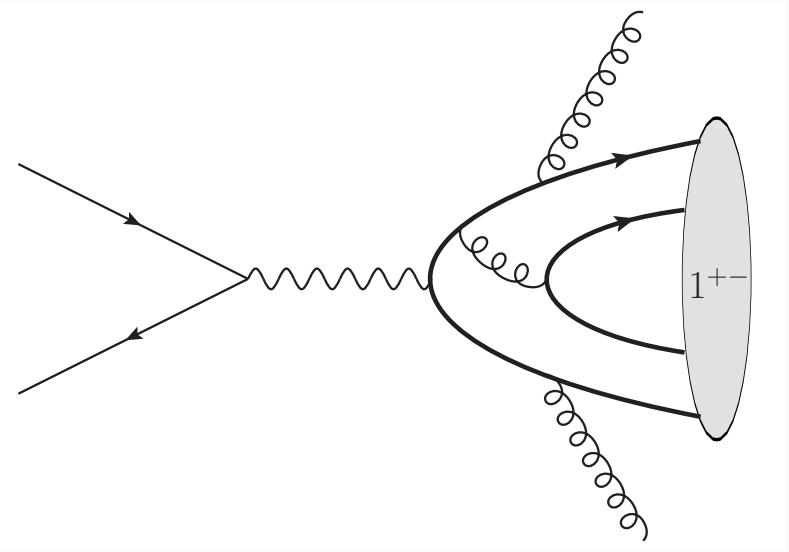

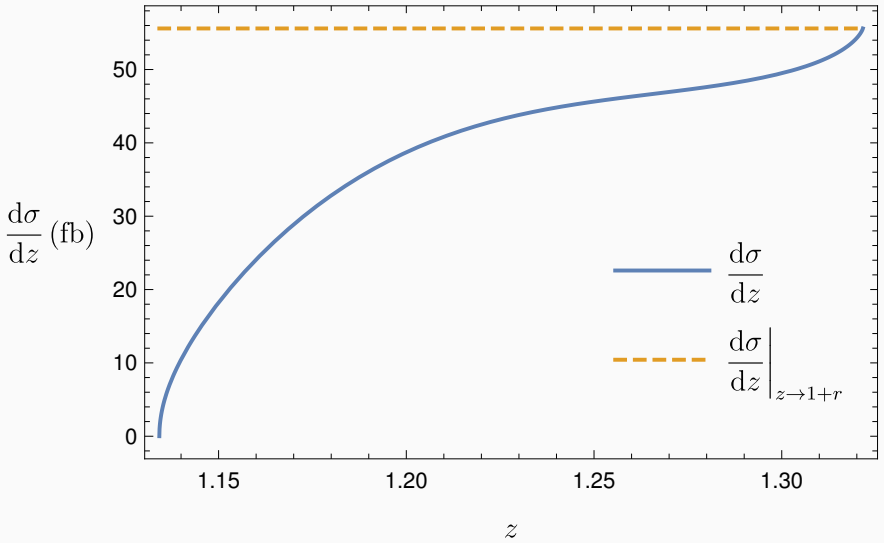

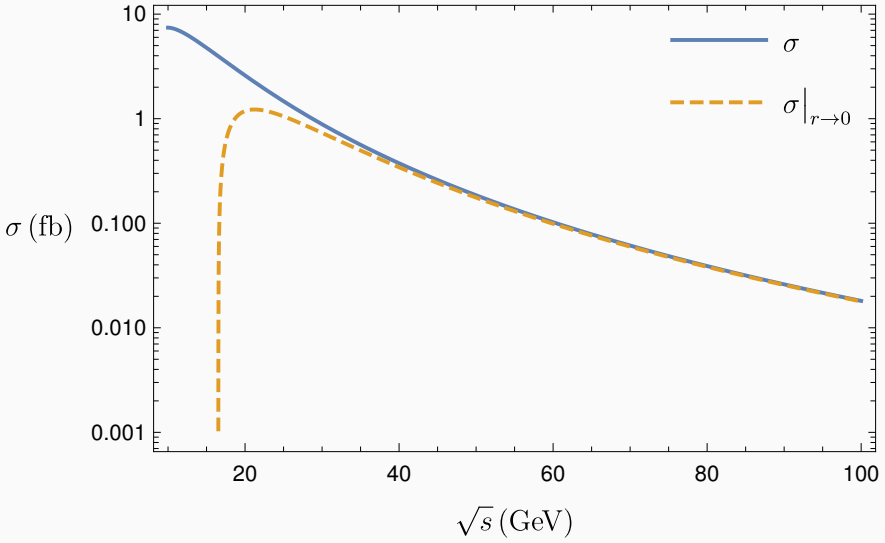

Phenomenological Applications

LHC, Belle II, and EIC

EIC PHOTOPRODUCTION

Study C-odd T_{4c}^1 with $\gamma + g$ in photoproduction at the EIC, with effective photon approximation

Factorization

$$\frac{\mathrm{d}\sigma}{\mathrm{d}z\,\mathrm{d}p_T} = \sum_i \int_{x_\gamma^{\min}}^1 \mathrm{d}x_\gamma \, \frac{2x_i p_T}{z(1-z)} \, f_{\gamma/e}(x_\gamma) f_{i/p}(x_i,\mu) \frac{\mathrm{d}\hat{\sigma}(\gamma + i \to T_{4c}^1 + j;\mu)}{\mathrm{d}\hat{t}}$$

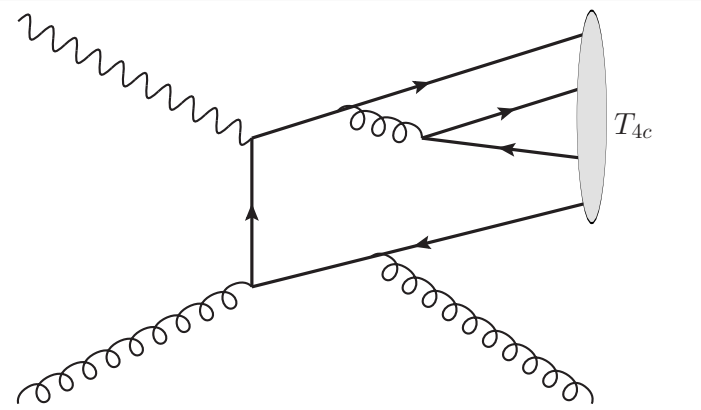

Feng, YH, Jia et al., PRD 110, 054007 (2024)

EIC Figure 2 p_T spectra at proposed EIC energies

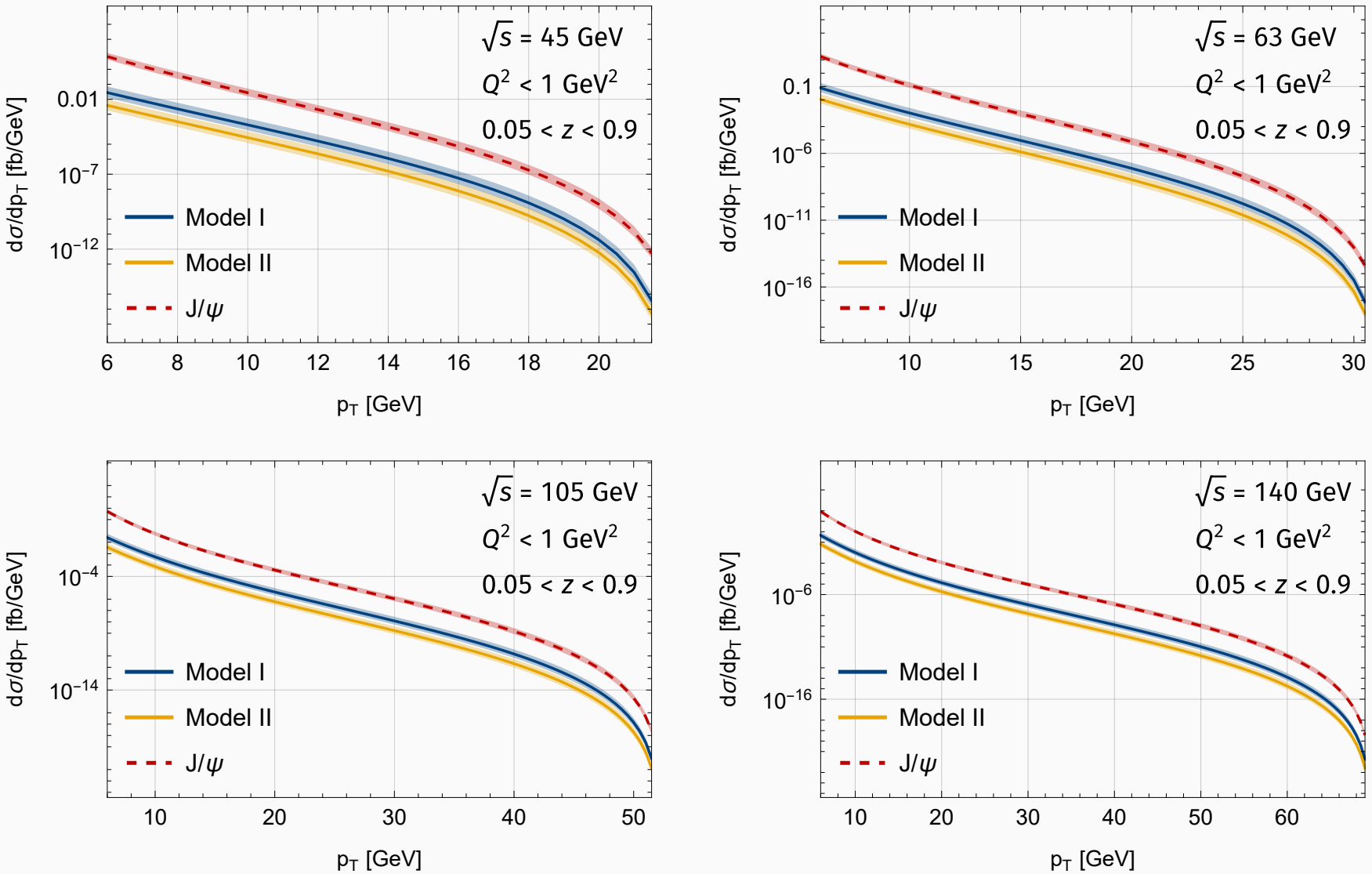

Feng, YH, Jia et al., PRD 110, 054007 (2024)

EIC Figure 3 p_T spectra at HERA and EicC

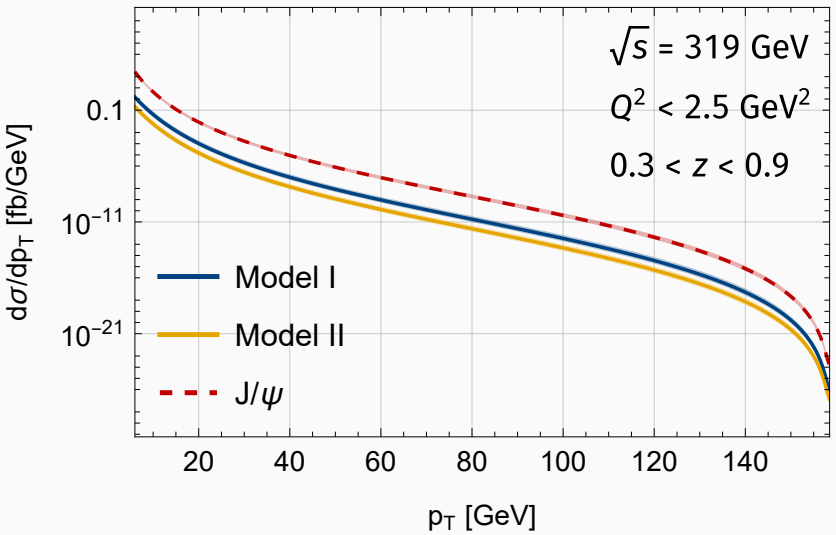

HERA

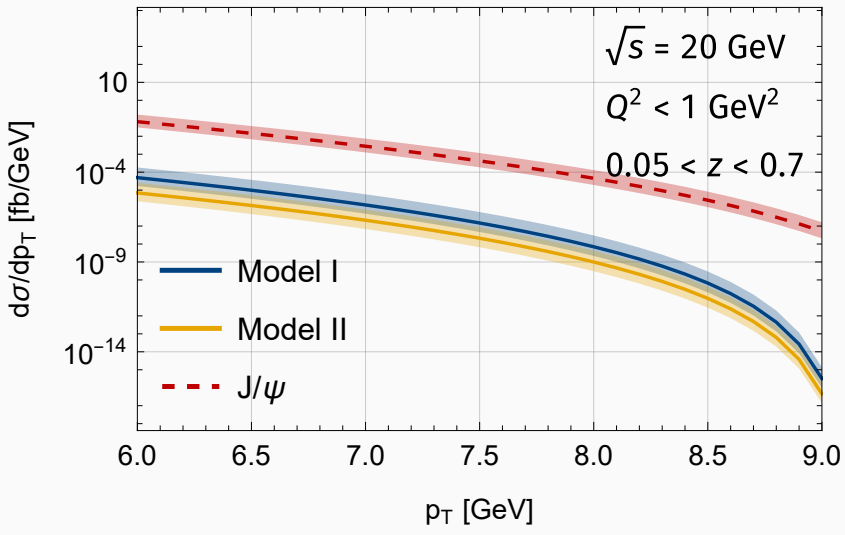

EicC

The next table quantifies the contrast: HERA has the larger cross section but little integrated luminosity, while EicC is strongly phase-space limited.

Feng, YH, Jia et al., PRD 110, 054007 (2024)

EIC Integrated rates and yields

setup	$\sqrt{s}$ [GeV]	E_p [GeV]	E_e [GeV]	p_T range [GeV]	σ_{I} [fb]	N_{I}	σ_{II} [fb]	N_{II}
EIC	44.7	100	5	6–20	0.022	2.2	0.0031	0.31
EIC	63.2	100	10	6–20	0.069	6.9	0.0098	0.98
EIC	104.9	275	10	6–20	0.25	25	0.035	3.5
EIC	140.7	275	18	6–20	0.45	45	0.064	6.4
HERA	319	920	27.5	6–20	1.5	0.72	0.22	0.10
EicC	20	19.08	5	6–9	1.5×10^{-5}	7.6×10^{-4}	2.1×10^{-6}	1.1×10^{-4}

Luminosities: EIC $100\,\mathrm{fb}^{-1}$/yr, HERA $468\,\mathrm{pb}^{-1}$, and EicC $50.5\,\mathrm{fb}^{-1}$/yr.
model I & II (II & III in the gluon fragmentation slide) are considered

Feng, YH, Jia et al., PRD 110, 054007 (2024)

EIC FRAGMENTATION COMPARISON

- The same fragmentation functions can be folded with EIC partonic production.

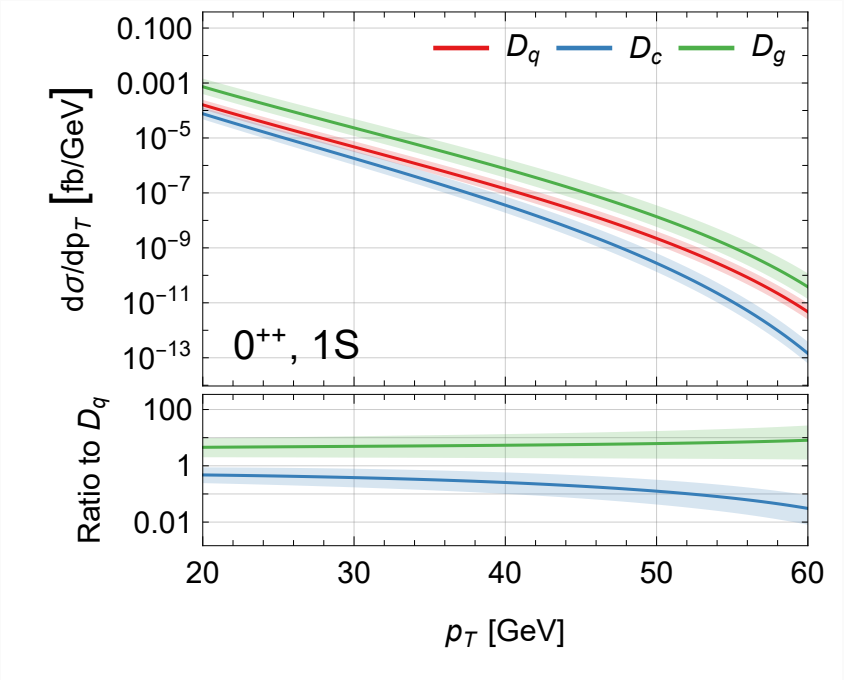

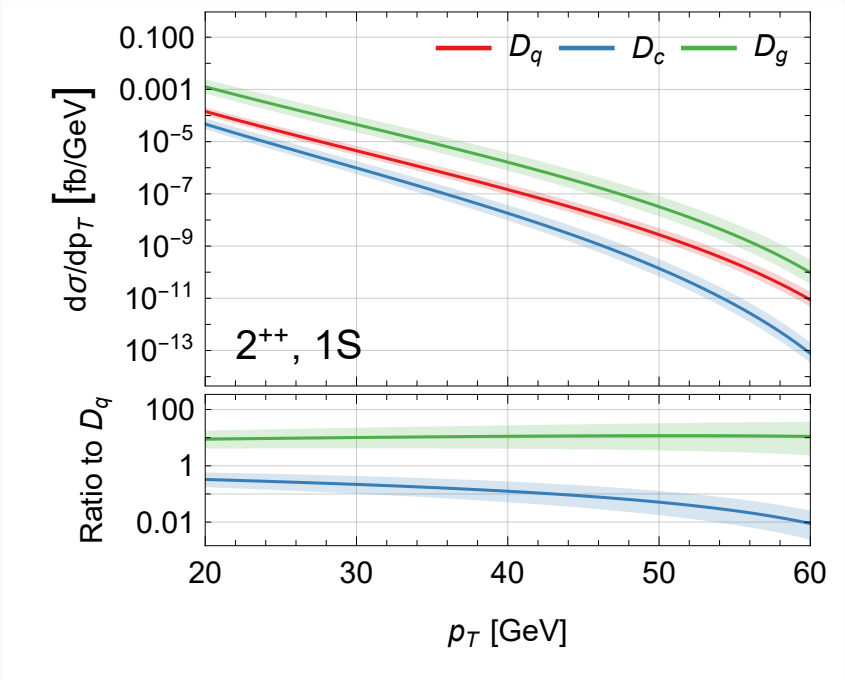

Bai, Feng, YH et al., JHEP 09, 002 (2024); Bai, YH & Sang, PRD 111, 054006 (2025)

Summary

Summary

- NRQCD factorization extends the quarkonium SDC/LDME logic to compact fully-heavy tetraquarks through local four-heavy-quark operators.
- At the LHC, fragmentation controls the high-p_T tail, while fixed-order production is essential at moderate p_T below $20\,\mathrm{GeV}$.
- Belle II, EIC, HERA & EicC remains inprobable to detect T_{4c}, but Belle II & EIC have better chances.

Main bottleneck

Better LDMEs, ideally from lattice QCD or future data, remain the key step for turning this framework into precision phenomenology.

Backup

The **SDCs** are insensitive to IR behaviors:

1. Replace physical (bounded) tetraquark state $\left|T_{4c}^{J}\right\rangle$ with a free 4-quark state $|cc\bar{c}\bar{c}\rangle$:

(VSA applied)
$$D_{g\to \cancel{T_{4c}}}(z,\mu_\Lambda)=\frac{d_{3,3}\left[g\to cc\bar{c}\bar{c}^{(J)}\right]}{m^9}\left|\left\langle \cancel{T_{4c}^{J}}\middle|\mathcal{O}^{(J)}_{\bar{\mathbf{3}}\otimes\mathbf{3}}\middle|0\right\rangle\right|^2+\cdots$$
$$\Rightarrow D_{g\to cc\bar{c}\bar{c}}(z,\mu_\Lambda)=\frac{d_{3,3}\left[g\to cc\bar{c}\bar{c}^{(J)}\right]}{m^9}\left|\langle cc\bar{c}\bar{c}|\mathcal{O}^{(J)}_{\bar{\mathbf{3}}\otimes\mathbf{3}}|0\rangle\right|^2+\cdots$$

   - For simplicity, we choose the angular momentum eigenstates of the free 4-quark states.

2. Perturbatively calculate both sides of the factorization formula (with QCD and NRQCD)
3. Solve the factorization formula to determine the **SDCs**

- Free four-quark states are constructed in angular momentum eigenstates
- Take the $\bar{\mathbf{3}} \otimes \mathbf{3}$ component as an example:
  - Free diquark state marked as $\left|\mathcal{D}^{\text{spin}}_{\text{color}}(P)\right\rangle$:

$$|\mathcal{D}^{s}_{c}(P)\rangle = \frac{1}{\sqrt{2}} \sum_{\lambda_1 \lambda_2} \left\langle \frac{1}{2}\lambda_1 \frac{1}{2}\lambda_2 \middle| 1s \right\rangle \frac{\epsilon^{abc}}{\sqrt{2}} \left| c_a^{\lambda_1}\left(\frac{P}{2}\right) c_b^{\lambda_2}\left(\frac{P}{2}\right) \right\rangle$$

  - Free tetraquark state marked as $\left|\mathcal{T}^{\text{spin}}_{\text{color}}(P)\right\rangle$:

$$\left|\mathcal{T}^{J,m_j}_{\bar{\mathbf{3}}\otimes\mathbf{3}}(Q)\right\rangle = \sum_{s_1 s_2} \langle 1 s_1 1 s_2 | J m_j \rangle \frac{\delta^{ab}}{\sqrt{3}} \left|\mathcal{D}^{s_1}_{a}\left(\frac{Q}{2}\right)\right\rangle \left|\overline{\mathcal{D}}^{s_2}_{b}\left(\frac{Q}{2}\right)\right\rangle$$

  - All states are non-relativistically normalized.

Values of NRQCD LDMEs

Different models give very distinct values and relative signs

- Model I: **Zhao:2020nwy**

$$\boxed{\langle 0|\mathcal{O}^{(0)}_{\bar{\mathbf{3}}\otimes\mathbf{3}}|T^0_{4c}\rangle \approx +2.402}, \qquad \boxed{\langle 0|\mathcal{O}^{(0)}_{\mathbf{6}\otimes\bar{\mathbf{6}}}|T^0_{4c}\rangle \approx +2.085}$$

$$\langle 0|\mathcal{O}^{(1)i}_{\bar{\mathbf{3}}\otimes\mathbf{3}}|T^1_{4c}\rangle \approx 2.31684\varepsilon^i, \qquad \langle 0|\mathcal{O}^{(2),\alpha\beta}_{\bar{\mathbf{3}}\otimes\mathbf{3}}|T^2_{4c}\rangle \approx 1.865\varepsilon^{\alpha\beta}$$

- Model II: **Lu:2020cns**

$$\boxed{\langle 0|\mathcal{O}^{(0)}_{\bar{\mathbf{3}}\otimes\mathbf{3}}|T^0_{4c}\rangle \approx -0.1864}, \qquad \boxed{\langle 0|\mathcal{O}^{(0)}_{\mathbf{6}\otimes\bar{\mathbf{6}}}|T^0_{4c}\rangle \approx -0.1132}$$

$$\langle 0|\mathcal{O}^{(1)i}_{\bar{\mathbf{3}}\otimes\mathbf{3}}|T^1_{4c}\rangle \approx -0.1612\varepsilon^i, \qquad \langle 0|\mathcal{O}^{(2),\alpha\beta}_{\bar{\mathbf{3}}\otimes\mathbf{3}}|T^2_{4c}\rangle \approx 0.1200\varepsilon^{\alpha\beta}$$

- Model III: **Liu:2020eha**

$$\boxed{\langle 0|\mathcal{O}^{(0)}_{\bar{\mathbf{3}}\otimes\mathbf{3}}|T^0_{4c}\rangle \approx -0.136737}, \qquad \boxed{\langle 0|\mathcal{O}^{(0)}_{\mathbf{6}\otimes\bar{\mathbf{6}}}|T^0_{4c}\rangle \approx +0.117944}$$

$$\langle 0|\mathcal{O}^{(1)i}_{\bar{\mathbf{3}}\otimes\mathbf{3}}|T^1_{4c}\rangle \approx 0.126437\varepsilon^i, \qquad \langle 0|\mathcal{O}^{(2),\alpha\beta}_{\bar{\mathbf{3}}\otimes\mathbf{3}}|T^2_{4c}\rangle \approx 0.112084\varepsilon^{\alpha\beta}$$